

Fast and Robust Spectrally Sparse Signal Recovery: A Provable Non-Convex Approach via Robust Low-Rank Hankel Matrix Reconstruction

HanQin Cai¹, Jian-Feng Cai², Tianming Wang³, and Guojian Yin⁴

¹Department of Mathematics, University of California, Los Angeles, Los Angeles, California, USA.

^{2,4}Department of Mathematics, Hong Kong University of Science and Technology, Clear Water Bay, Kowloon, Hong Kong SAR, China.

³Institute for Computational Engineering and Sciences, University of Texas at Austin, Austin, Texas, USA.

October 29, 2021

Abstract

Consider a spectrally sparse signal \mathbf{x} that consists of r complex sinusoids with or without damping. We study the robust recovery problem for the spectrally sparse signal under the fully observed setting, which is about recovering \mathbf{x} and a sparse corruption vector \mathbf{s} from their sum $\mathbf{z} = \mathbf{x} + \mathbf{s}$. In this paper, we exploit the low-rank property of the Hankel matrix constructed from \mathbf{x} , and develop an efficient non-convex algorithm, coined Accelerated Alternating Projections for Robust Low-Rank Hankel Matrix Reconstruction (AAP-Hankel). The high computational efficiency and low space complexity of AAP-Hankel are achieved by fast computations involving structured matrices, and a subspace projection method for accelerated low-rank approximation. Theoretical recovery guarantee with a linear convergence rate has been established for AAP-Hankel. Empirical performance comparisons on synthetic and real-world datasets demonstrate the computational advantages of AAP-Hankel, in both efficiency and robustness aspects.

1 Introduction

In this paper, we study the corrupted spectrally sparse signal recovery problem under the fully observed setting. Denote the imaginary unit by \imath . Let $x(t)$ be a continuous one-dimensional spectrally r -sparse signal; that is, $x(t)$ is a weighted superposition of r complex sinusoids

$$x(t) = \sum_{j=1}^r a_j e^{2\pi\imath f_j t - d_j t}, \quad (1)$$

Email addresses: hqcai@math.ucla.edu (H.Q. Cai), jfcai@ust.hk (J.-F. Cai), tw27479@utexas.edu (T. Wang, corresponding author), and magjiyin@ust.hk (G. Yin).

where a_j , f_j and d_j represent non-zero complex amplitude, normalized frequency and damping factor of the j^{th} sinusoid, respectively. Furthermore, let column vector

$$\mathbf{x} = [x(0), x(1), \dots, x(n-1)]^T \in \mathbb{C}^n \quad (2)$$

denote the discrete samples of $x(t)$.

The spectrally sparse signal, as defined in (1), appears in a wide range of applications, including seismic imaging [1], analog-to-digital conversion [2; 3], nuclear magnetic resonance (NMR) spectroscopy [4; 5; 6], and fluorescence microscopy [7]. Due to malfunction of data acquisition sensors, the recorded signals are often corrupted by impulse noise, e.g., baseline distortions in NMR [8]. Since the amount of impulse noise corruptions is often relatively small compared to the signal size, we can consider them as sparse corruptions. It is thus of importance to remove such sparse corruptions and recover the original signal accurately.

1.1 Model and Assumptions

Suppose we receive a corrupted signal $\mathbf{z} \in \mathbb{C}^n$, which is the sum of an underlying spectrally sparse signal and some sparse corruptions, namely $\mathbf{z} = \mathbf{x} + \mathbf{s}$. Then, our goal is to recover \mathbf{x} and \mathbf{s} from \mathbf{z} simultaneously. This vector separating problem can be expressed as:

$$\min_{\mathbf{x}', \mathbf{s}'} \|\mathbf{z} - \mathbf{x}' - \mathbf{s}'\|_2^2 \quad \text{subject to } \mathbf{x}' \text{ is spectrally sparse and } \mathbf{s}' \text{ is sparse;} \quad (3)$$

that is, we are seeking a spectrally sparse vector \mathbf{x}' and sparse vector \mathbf{s}' such that their sum fits best to the given vector \mathbf{z} . However, a corrupted signal cannot be fully recovered unless it has certain inherent structure that provides a unique determination of the corrupted entries. Inspired by robust principal component analysis (RPCA) [9; 10; 11], which recovers a low-rank matrix from corruptions under some natural conditions, we exploit the low-rank property of the Hankel matrix constructed from a spectrally sparse signal in this paper.

Let $\mathcal{H} : \mathbb{C}^n \rightarrow \mathbb{C}^{n_1 \times n_2}$ denote a mapping from a complex vector to a complex Hankel matrix, where $n = n_1 + n_2 - 1$. For any vector $\mathbf{v} = [v_0; v_1; \dots; v_{n-1}] \in \mathbb{C}^n$, we define

$$\mathcal{H}(\mathbf{v}) = \begin{bmatrix} v_0 & v_1 & v_2 & \cdots & v_{n_2-1} \\ v_1 & v_2 & v_3 & \cdots & v_{n_2} \\ \vdots & \vdots & \vdots & \cdots & \vdots \\ v_{n_1-1} & v_{n_1} & v_{n_1+1} & \cdots & v_{n-1} \end{bmatrix} \in \mathbb{C}^{n_1 \times n_2}. \quad (4)$$

Here a good choice of the matrix size is $n_1 \approx n_2$, i.e., we want to construct a nearly squared Hankel matrix. Without loss of generality, throughout this paper, we will use $n_1 = n_2 = (n+1)/2$ if n is odd, and $n_1 = n_2 - 1 = n/2$ if otherwise.

Suppose $\mathbf{x} \in \mathbb{C}^n$ is a spectrally r -sparse signal, then we can get a Vandermonde decomposition of $\mathcal{H}(\mathbf{x})$ in the form of

$$\mathcal{H}(\mathbf{x}) = \mathbf{E}_L \mathbf{D} \mathbf{E}_R^T,$$

where $\mathbf{D} = \text{diag}([a_1, a_2, \dots, a_r])$, $[\mathbf{E}_L]_{i_1, j} = \omega_j^{i_1-1}$, $[\mathbf{E}_R]_{i_2, j} = \omega_j^{i_2-1}$, and $\omega_j = e^{2\pi i f_j - d_j}$ for $i_1 \in \{1, \dots, n_1\}$, $i_2 \in \{1, \dots, n_2\}$ and $j \in \{1, \dots, r\}$. It is easy to see that the left and right matrices in this Vandermonde decomposition are both of full rank. Thus, $\mathcal{H}(\mathbf{x})$ is rank- r provided all the complex amplitudes $\{a_j\}$ are non-zero. It is worth mentioning that the low-rank Hankel matrix

also appears in many other applications, such as magnetic resonance imaging (MRI) [12; 13; 14], dynamical system identification [15; 16], and autoregressive moving average (ARMA) [17; 18]. Corruptions also often appear in these applications, e.g., Herringbone artifact in MRI [19].

Furthermore, given a sparse vector \mathbf{s} that has no more than m non-zero entries, then by the definition, $\mathcal{H}(\mathbf{s})$ has no more than m non-zero entries per row and column. In other words, if the vector \mathbf{s} is sparse, then the Hankel matrix $\mathcal{H}(\mathbf{s})$ is sparse as well.

With the properties of Hankel operator \mathcal{H} , we can reformulate the corrupted spectrally sparse signal recovery problem (3) to a robust low-rank Hankel matrix reconstruction problem

$$\min_{\mathbf{x}', \mathbf{s}'} \|\mathcal{H}(\mathbf{z}) - \mathcal{H}(\mathbf{x}') - \mathcal{H}(\mathbf{s}')\|_F^2 \quad \text{subject to } \text{rank}(\mathcal{H}(\mathbf{x}')) = r \text{ and } \|\mathbf{s}'\|_0 \leq |\Omega|, \quad (5)$$

where $\|\cdot\|_F$ denotes the Frobenius norm of matrices, $\|\cdot\|_0$ counts the number of non-zero entries, and Ω denotes the support set of the underlying corruptions. Note that \mathcal{H} is an injective mapping; hence, the reconstruction of \mathbf{x} and $\mathcal{H}(\mathbf{x})$ are equivalent.

Without any further assumptions, the optimization problem (5) is clearly ill-posed. For successful reconstruction, we assume that $\mathcal{H}(\mathbf{x})$ is not too sparse, and \mathbf{s} is not too dense. We formalize these assumptions as A1 and A2.

A1 The underlying Hankel matrix $\mathcal{H}(\mathbf{x}) \in \mathbb{C}^{n_1 \times n_2}$ is rank- r with μ -incoherence, that is

$$\max_i \|e_i^T \mathbf{U}\|_2 \leq \sqrt{\frac{\mu c_s r}{n}}, \quad \text{and} \quad \max_j \|e_j^T \mathbf{V}\|_2 \leq \sqrt{\frac{\mu c_s r}{n}} \quad (6)$$

where $c_s := \max\{n/n_1, n/n_2\}$, and $\mathbf{U}\mathbf{\Sigma}\mathbf{V}^*$ is the singular value decomposition (SVD) of $\mathcal{H}(\mathbf{x})$.

Theoretically, A1 holds if the minimum warp-around distances between each pair of the frequencies $\{f_j\}$ are greater than $2/n$ in the undamped case [20, Theorem 2]. Empirically, we found that A1 is commonly satisfied in random spectrally sparse signals and real-world examples, with or without damping factors.

A2 The corruption vector $\mathbf{s} \in \mathbb{C}^n$ is α -sparse, i.e., \mathbf{s} has at most αn non-zero entries. This implies that $\mathcal{H}(\mathbf{s})$ has at most αn non-zero entries per each row and column. In this paper, we assume

$$\alpha \leq O\left(\min\left\{\frac{1}{\mu c_s r^2 \kappa^3}, \frac{1}{\mu^{1.5} c_s^{1.5} r^2 \kappa}, \frac{1}{\mu^2 c_s^2 r^2}\right\}\right), \quad (7)$$

where $\kappa := \sigma_1(\mathcal{H}(\mathbf{x}))/\sigma_r(\mathcal{H}(\mathbf{x}))$ is the condition number of $\mathcal{H}(\mathbf{x})$.

Essentially, A2 states that there cannot be too many corruptions in the corrupted signal. Note that we make no assumption on the distribution of the corruptions since $\mathcal{H}(\mathbf{s})$ preserves the sparsity of \mathbf{s} . Additionally, if the minimum warp-around distances are greater than $2/n$, then the condition number κ of the corresponding Hankel matrix is bound by $O(1)$ [20, Remark 1].

1.2 Prior Art and Contributions

Most early works of robust spectrally sparse signal recovery aim at solving (3). For undamped signal whose frequencies are lying on the grids, the ℓ_1 minimization based robust compressed sensing approach can successfully recover the original signal from corruptions [21]; however, the performance of these approaches degrade if there is mismatch between the assumed frequency basis

and the true basis [22]. To handle the off-the-grid situation, [23] proposes an approach based on total-variation norm minimization that can remove corruptions from signal when the signal frequencies are sufficiently separated. Its theoretical results rely on the assumption that phases of the amplitude of the signal and the sparse components are uniform distributed. The total-variation based minimization requires solving a SDP, which is computationally expensive in general. Hankel formulation is another way to handle the off-the-grid frequencies with an additional advantage to be able to model damping in the signals appeared in, e.g., NMR. Methods based on Hankel formulation aim at solving problems similar as (5).

In [24], a convex method Robust-EMaC is introduced with guaranteed recovery. It penalizes nuclear norm to enforce the low-rank property of $\mathcal{H}(\mathbf{x}')$ and elementwise ℓ_1 norm to promote the sparsity of $\mathcal{H}(\mathbf{s}')$. Its original formulation also requires solving a SDP. Even employing a first-order solver, it generally costs $O(n^2 \log(n))$ flops per iteration. More recently, a non-convex algorithm named SAP has been proposed in [25]. SAP projects the estimates of $\mathcal{H}(\mathbf{x})$ and \mathbf{s} onto the set of low rank matrices and the set of sparse vectors alternatively; to void the potential negative effect from ill-conditioned matrices, SAP gradually increase the effective rank from 1 to r . SAP is equipped with guaranteed linear convergence and costs $O(r^2 n \log(n) \log(1/\epsilon))$ flops to achieve an accuracy of ϵ , where the hidden constant is large and depends on the relative gaps between the singular values of $\mathcal{H}(\mathbf{x})$. In contrast, our method costs only $O((r^2 n + r n \log(n)) \log(1/\epsilon))$ flops to achieve the same accuracy, where the hidden constant is a fixed small number.

Our main contributions are two-fold. Firstly, we introduce a new non-convex algorithm, coined Accelerated Alternating Projections for Robust Low-Rank Hankel Matrix Reconstruction (AAP-Hankel), for robust spectrally sparse signal recovery problem. AAP-Hankel has state-of-the-art computational efficiency and robustness, which are demonstrated by empirical performance comparisons. Secondly, we establish the theoretical exact recovery for AAP-Hankel. That is, AAP-Hankel can recover a spectrally sparse signals assuredly provided the corruptions are sufficiently sparse. It is worth mentioning that our algorithm and theoretical results apply to general low-rank Hankel matrices arise from applications, though we focus on the Hankel matrices constructed from spectrally sparse signals in this work.

1.3 Notation and Organization

In this paper, we denote column vectors by bold lowercase letters (e.g., \mathbf{v}), matrices by bold capital letters (e.g., \mathbf{M}), and operators by calligraphic letters (e.g., \mathcal{P}). For any vector \mathbf{v} , $\|\mathbf{v}\|_2$ and $\|\mathbf{v}\|_\infty$ denotes the ℓ_2 norm and ℓ_∞ norm of \mathbf{v} , respectively. For any matrix \mathbf{M} , $[\mathbf{M}]_{i,j}$ denotes its $(i,j)^{th}$ entry, $\sigma_i(\mathbf{M})$ and σ_i^M denote its i^{th} singular value, $\|\mathbf{M}\|_\infty = \max_{i,j} |[\mathbf{M}]_{i,j}|$ denotes the maximum magnitude among its entries, $\|\mathbf{M}\|_2 = \sigma_1(\mathbf{M})$ denotes its spectral norm, $\|\mathbf{M}\|_F = \sqrt{\sum_i \sigma_i^2(\mathbf{M})}$ denotes its Frobenius norm, and $\|\mathbf{M}\|_* = \sum_i \sigma_i(\mathbf{M})$ denotes its nuclear norm. Furthermore, for any vector or matrix, $\langle \cdot, \cdot \rangle$, $\overline{(\cdot)}$, $(\cdot)^T$, and $(\cdot)^*$ denote the inner product, conjugate, transpose and conjugate transpose, respectively.

In particular, we use \mathbf{e}_i to denote the i^{th} canonical basis vector, \mathbf{I} to denote the identity matrix, and \mathcal{I} to denote the identity operator. Additionally, through this paper, $\mathbf{L} = \mathcal{H}(\mathbf{x})$ always denote the underlying rank- r Hankel matrix, $\kappa = \sigma_1^L / \sigma_r^L$ always denotes the condition number of \mathbf{L} , and $\Omega = \text{supp}(\mathbf{s})$ is always referred to as the support of the underlying sparse corruption vector \mathbf{s} . At the k^{th} iteration, the estimates of \mathbf{L} , \mathbf{x} and \mathbf{s} are denoted by \mathbf{L}_k , \mathbf{x}_k and \mathbf{s}_k , respectively.

We organize the rest of the paper as follows. Sections 2.1 and 2.2 present the proposed main algorithm and corresponding initialization, respectively. The theoretical results of the proposed

algorithms are presented in Section 2.3, followed by an extended discussion on multi-dimensional signals. Section 3 contains the numerical simulations of our algorithms, on both synthetic and real-world datasets. All the mathematical proofs of our theoretical results are presented in Section 4. The paper is concluded with future directions in Section 5.

2 Algorithms

It is clear that robust low-rank Hankel matrix recovery problem (5) can be viewed as a RPCA problem, and we can solve it with any off-the-shelf RPCA algorithm. However, without taking advantage of Hankel structure, we cannot achieve the optimal computational efficiency and robustness. Inspired by an accelerated alternating projections (AccAltProj) algorithm for RPCA introduced in [11], we present an accelerated algorithm for the problem (5), dubbed Accelerated Alternating Projections for Robust Low-Rank Hankel Matrix Reconstruction (AAP-Hankel). The new algorithm not only has state-of-the-art computational efficiency, but also retains theoretical guarantee of recovery.

The proposed algorithm proceeds in two phases. In the first phase, we initialize the algorithm by alternating projections for one step. In the second phase, we project $\mathcal{H}(\mathbf{z} - \mathbf{s})$ onto the space of rank- r matrices with an accelerated method, update the estimate of \mathbf{x} correspondingly, and project $\mathbf{z} - \mathbf{x}$ onto the space of sparse vectors to update the estimate of \mathbf{s} .

2.1 Main Algorithm

Algorithm 1 Accelerated Alternating Projections for Robust Low-Rank **H**ankel Matrix Reconstruction (AAP-Hankel)

- 1: **Input:** \mathbf{z} , observed corrupted signal; r , model order; ϵ , target precision level; β , thresholding parameter; γ , target converge rate; μ , incoherence parameter.
 - 2: **Initialization** and set $k = 0$
 - 3: **while** $\|\mathbf{z} - \mathbf{x}_k - \mathbf{s}_k\|_2 / \|\mathbf{z}\|_2 \geq \epsilon$ **do**
 - 4: $\tilde{\mathbf{L}}_k = \text{Trim}(\mathbf{L}_k, \mu)$
 - 5: $\mathbf{L}_{k+1} = \mathcal{D}_r \mathcal{P}_{\tilde{T}_k} \mathcal{H}(\mathbf{z} - \mathbf{s}_k)$
 - 6: $\mathbf{x}_{k+1} = \mathcal{H}^\dagger(\mathbf{L}_{k+1})$
 - 7: $\zeta_{k+1} = \beta \left(\sigma_{r+1} \left(\mathcal{P}_{\tilde{T}_k} \mathcal{H}(\mathbf{z} - \mathbf{s}_k) \right) + \gamma^{k+1} \sigma_1 \left(\mathcal{P}_{\tilde{T}_k} \mathcal{H}(\mathbf{z} - \mathbf{s}_k) \right) \right)$
 - 8: $\mathbf{s}_{k+1} = \mathcal{T}_{\zeta_{k+1}}(\mathbf{z} - \mathbf{x}_{k+1})$
 - 9: $k = k + 1$
 - 10: **Output:** $\mathbf{x}_k, \mathbf{s}_k$
-

Firstly, we will discuss the second phase - the main algorithm, which is summarized in Algorithm 1. For ease of presentation, we denote $\mathbf{L} := \mathcal{H}(\mathbf{x})$ as the underlying low-rank Hankel matrix throughout the rest of the paper. Denote \mathbf{L}_k , \mathbf{x}_k and \mathbf{s}_k as the current estimates of low-rank Hankel matrix, spectrally sparse signal and corruptions, respectively.

At the $(k+1)^{th}$ iteration, we first employ Algorithm 2 to trim \mathbf{L}_k into a rank- r incoherent matrix $\tilde{\mathbf{L}}_k$. Then, we consider a low-dimensional subspace \tilde{T}_k formed by the direct sum of the column and

Algorithm 2 Trim

1: **Input:** $\mathbf{L} = \mathbf{U}\mathbf{\Sigma}\mathbf{V}^*$, matrix to be trimmed; μ , target incoherence level.
 2: $c_\mu = \sqrt{\frac{\mu c_s r}{n}}$
 3: **for** $i = 1$ **to** n_1 **do**
 4: $[\mathbf{A}]_{i,:} = \min\{1, c_\mu / \|\mathbf{U}\|_{i,:}\|_2\} \cdot [\mathbf{U}]_{i,:}$
 5: **for** $j = 1$ **to** n_2 **do**
 6: $[\mathbf{B}]_{j,:} = \min\{1, c_\mu / \|\mathbf{V}\|_{j,:}\|_2\} \cdot [\mathbf{V}]_{j,:}$
 7: **Output:** $\tilde{\mathbf{L}} = \mathbf{A}\mathbf{\Sigma}\mathbf{B}^*$

row spaces of $\tilde{\mathbf{L}}_k$, i.e.,

$$\tilde{T}_k = \left\{ \tilde{\mathbf{U}}_k \mathbf{A}^* + \mathbf{B} \tilde{\mathbf{V}}_k^* \mid \mathbf{A} \in \mathbb{C}^{n_2 \times r}, \mathbf{B} \in \mathbb{C}^{n_1 \times r} \right\}, \quad (8)$$

where $\tilde{\mathbf{L}}_k = \tilde{\mathbf{U}}_k \tilde{\mathbf{\Sigma}}_k \tilde{\mathbf{V}}_k^*$ is its SVD. The subspace \tilde{T}_k can be viewed as the tangent space of the rank- r matrix manifold at $\tilde{\mathbf{L}}_k$ [26], and it has been widely studied in the low-rank matrices related recovery problems [27; 28; 29; 30; 31]. Moreover, for any $\mathbf{M} \in \mathbb{C}^{n_1 \times n_2}$, the projection of \mathbf{M} onto the low-dimensional subspace \tilde{T}_k is computed by

$$\mathcal{P}_{\tilde{T}_k} \mathbf{M} = \tilde{\mathbf{U}}_k \tilde{\mathbf{U}}_k^* \mathbf{M} + \mathbf{M} \tilde{\mathbf{V}}_k \tilde{\mathbf{V}}_k^* - \tilde{\mathbf{U}}_k \tilde{\mathbf{U}}_k^* \mathbf{M} \tilde{\mathbf{V}}_k \tilde{\mathbf{V}}_k^*. \quad (9)$$

Note that for the low-dimensional subspace projection $\mathcal{P}_{\tilde{T}_k}$, we only need the trimmed singular vectors $\tilde{\mathbf{U}}_k$ and $\tilde{\mathbf{V}}_k$, which can be computed efficiently via QR-decompositions.

To get new estimate \mathbf{L}_{k+1} , we first project Hankel matrix $\mathcal{H}(\mathbf{z} - \mathbf{s}_k)$ onto the low-dimensional subspace \tilde{T}_k , then project from this subspace onto the set of rank- r matrices. That is,

$$\mathbf{L}_{k+1} = \mathcal{D}_r \mathcal{P}_{\tilde{T}_k} \mathcal{H}(\mathbf{z} - \mathbf{s}_k), \quad (10)$$

where \mathcal{D}_r computes the nearest rank- r approximation via truncated SVD. Though there is a SVD in this step, we can compute it efficiently by using the properties of the low-dimensional subspace \tilde{T}_k [26; 31; 11; 32]. Denote $\mathbf{H}_k := \mathcal{H}(\mathbf{z} - \mathbf{s}_k)$. Let $(\mathbf{I} - \tilde{\mathbf{V}}_k \tilde{\mathbf{V}}_k^*) \mathbf{H}_k^* \tilde{\mathbf{U}}_k = \mathbf{Q}_1 \mathbf{R}_1$ and $(\mathbf{I} - \tilde{\mathbf{U}}_k \tilde{\mathbf{U}}_k^*) \mathbf{H}_k \tilde{\mathbf{V}}_k = \mathbf{Q}_2 \mathbf{R}_2$ be the QR-decompositions. Noticing $\tilde{\mathbf{V}}_k \perp \mathbf{Q}_1$ and $\tilde{\mathbf{U}}_k \perp \mathbf{Q}_2$, we have

$$\mathcal{P}_{\tilde{T}_k} \mathbf{H}_k = \begin{bmatrix} \tilde{\mathbf{U}}_k & \mathbf{Q}_1 \end{bmatrix} \mathbf{M}_k \begin{bmatrix} \tilde{\mathbf{V}}_k & \mathbf{Q}_2 \end{bmatrix}^*, \quad (11)$$

where $\mathbf{M}_k := \begin{bmatrix} \tilde{\mathbf{U}}_k^* \mathbf{H}_k \tilde{\mathbf{V}}_k & \mathbf{R}_2^* \\ \mathbf{R}_1 & \mathbf{0} \end{bmatrix}$ is a $2r \times 2r$ matrix. Let $\mathbf{M}_k = \mathbf{U}_{M_k} \mathbf{\Sigma}_{M_k} \mathbf{V}_{M_k}^*$ be the SVD of \mathbf{M}_k . Since both $\begin{bmatrix} \tilde{\mathbf{U}}_k & \mathbf{Q}_1 \end{bmatrix}$ and $\begin{bmatrix} \tilde{\mathbf{V}}_k & \mathbf{Q}_2 \end{bmatrix}$ are orthonormal, we can obtain the SVD of $\mathcal{P}_{\tilde{T}_k} \mathbf{H}_k = \tilde{\mathbf{U}}_{k+1} \tilde{\mathbf{\Sigma}}_{k+1} \tilde{\mathbf{V}}_{k+1}^*$ by

$$\tilde{\mathbf{U}}_{k+1} = \begin{bmatrix} \tilde{\mathbf{U}}_k & \mathbf{Q}_1 \end{bmatrix} \mathbf{U}_{M_k}, \quad \tilde{\mathbf{\Sigma}}_{k+1} = \mathbf{\Sigma}_{M_k}, \quad \text{and} \quad \tilde{\mathbf{V}}_{k+1} = \begin{bmatrix} \tilde{\mathbf{V}}_k & \mathbf{Q}_2 \end{bmatrix} \mathbf{V}_{M_k}. \quad (12)$$

The truncated SVD of $\mathcal{P}_{\tilde{T}_k} \mathcal{H}(\mathbf{z} - \mathbf{s}_k)$ then follows. Altogether, the computational cost of (10) is dominated by the multiplication between a $n_1 \times n_2$ Hankel matrix and a $n_2 \times r$ matrix, the

multiplication between a $n_2 \times n_1$ Hankel matrix and a $n_1 \times r$ matrix, two QR-decompositions of sizes $n_1 \times r$ and $n_2 \times r$, and a small SVD of a $2r \times 2r$ matrix. The Hankel matrix-vector multiplication can be computed efficiently without forming the Hankel matrix explicitly via fast convolution, which costs only $O(n \log(n))$ flops [33]. Hence, updating \mathbf{L} estimate requires $O(r^2 n + rn \log(n) + r^3)$ flops with a fixed small constant in the front.

Next, we will update the estimate of \mathbf{x} by applying the left inverse of Hankel mapping to the new estimate of \mathbf{L} . Let $\mathcal{H}^\dagger : \mathbb{C}^{n_1 \times n_2} \rightarrow \mathbb{C}^n$ denote the left inverse of \mathcal{H} . For any matrix $\mathbf{M} \in \mathbb{C}^{n_1 \times n_2}$ and $0 \leq t \leq n-1$,

$$[\mathcal{H}^\dagger(\mathbf{M})]_t = \frac{1}{\rho_t} \sum_{a+b=t} [\mathbf{M}]_{a,b}, \quad (13)$$

where ρ_t is the number of entries on the t -th anti-diagonal of \mathbf{M} . It is easy to verify that $\mathcal{H}^\dagger \mathcal{H} = \mathcal{I}$. Furthermore,

$$\mathbf{x}_{k+1} = \mathcal{H}^\dagger(\mathbf{L}_{k+1}) = \sum_{j=1}^r [\Sigma_{k+1}]_{j,j} \mathcal{H}^\dagger([\mathbf{U}_{k+1}]_{:,j} ([\mathbf{V}_{k+1}]_{:,j})^*), \quad (14)$$

where $[\mathcal{H}^\dagger([\mathbf{U}_{k+1}]_{:,j} ([\mathbf{V}_{k+1}]_{:,j})^*)]_t = \frac{1}{\rho_t} \sum_{a+b=t} [\mathbf{U}_{k+1}]_{a,j} [\overline{\mathbf{V}_{k+1}}]_{b,j}$, so it can be computed via fast convolution. Thus, the computational costs of (14) is $O(rn \log(n))$.

Although the first three steps of AAP-Hankel involve $n_1 \times n_2$ matrices, the entire process does not require forming these matrices explicitly. We only need to store the corresponding vector for the Hankel matrix and the SVD components for rank- r matrix. Therefore, the space complexity of AAP-Hankel is $O(rn)$ instead of $O(n^2)$.

After we obtain the new estimate of \mathbf{x} , AAP-Hankel updates the estimate of \mathbf{s} by projecting $\mathbf{z} - \mathbf{x}_{k+1}$ onto the space of sparse vectors via hard thresholding,

$$\mathbf{s}_{k+1} = \mathcal{T}_{\zeta_{k+1}}(\mathbf{z} - \mathbf{x}_{k+1}), \quad (15)$$

where \mathcal{T}_ζ is the hard thresholding operator with thresholding value ζ . The key to successful isolation of corruptions is the choice of proper thresholding values. At the $(k+1)^{th}$ iteration, AAP-Hankel selects the hard thresholding value as

$$\zeta_{k+1} = \beta \left(\sigma_{r+1} \left(\mathcal{P}_{\tilde{T}_k} \mathcal{H}(\mathbf{z} - \mathbf{s}_k) \right) \right) + \gamma^{k+1} \sigma_1 \left(\mathcal{P}_{\tilde{T}_k} \mathcal{H}(\mathbf{z} - \mathbf{s}_k) \right), \quad (16)$$

where β is a positive tuning parameter and $\gamma \in (0, 1)$ is a convergence rate parameter. Note that computing ζ_{k+1} involves the singular values of $\mathcal{P}_{\tilde{T}_k} \mathcal{H}(\mathbf{z} - \mathbf{s}_k)$, which have been computed in (10). Thus, the computational cost of ζ_{k+1} is negligible, and the total cost of updating \mathbf{s} is $O(n)$ flops.

2.2 Initialization

To apply the proposed acceleration method for rank- r matrix projection, i.e., (10), we need to form the low-dimensional subspace \tilde{T}_0 by the singular vectors of a reasonably estimated \mathbf{L}_0 . Thus, we propose an initialization method based on two-step alternating projections, which is summarized in Algorithm 3. The primary difference between initialization scheme and main algorithm is a full size truncated SVD, without acceleration by the subspace projection, when updating \mathbf{L}_0 . However, the matrix-vector multiplications involved in the truncated SVD of a Hankel matrix can be computed via fast convolution without forming the Hankel matrices explicitly; that is, the computational complexity of updating \mathbf{L}_0 is $O(rn \log(n))$ with a large hidden constant depending on the gaps

Algorithm 3 Initialization

- 1: **Input:** $\mathbf{z} = \mathbf{x} + \mathbf{s}$, observed signal; r , rank of $\mathcal{H}(\mathbf{x})$; β_{init} and β , thresholding parameters.
 - 2: $\mathbf{x}_{-1} = \mathbf{0}$
 - 3: $\zeta_{-1} = \beta_{init} \sigma_1(\mathcal{H}(\mathbf{z}))$
 - 4: $\mathbf{s}_{-1} = \mathcal{T}_{\zeta_{-1}}(\mathbf{z} - \mathbf{x}_{-1})$
 - 5: $\mathbf{L}_0 = \mathcal{D}_r \mathcal{H}(\mathbf{z} - \mathbf{s}_{-1})$
 - 6: $\mathbf{x}_0 = \mathcal{H}^\dagger(\mathbf{L}_0)$
 - 7: $\zeta_0 = \beta \sigma_1(\mathbf{L}_0)$
 - 8: $\mathbf{s}_0 = \mathcal{T}_{\zeta_0}(\mathbf{z} - \mathbf{x}_0)$
 - 9: **Output:** $\mathbf{L}_0, \mathbf{s}_0$.
-

between the singular values [34], and the space complexity remains $O(rn)$ as we only need to store the singular vectors of \mathbf{L}_0 . It is worth mentioning that when we make the initial guess of \mathbf{s} , a thresholding parameter β_{init} is used to offset the spectral perturbation caused by corruptions, which may be turned differently than β in Algorithm 1.

In summary, the overall space complexity of the new algorithm is $O(rn)$, the computational cost per iteration is $O(r^2n + rn \log(n))$ flops with fixed small hidden constant, and additional $O(rn \log(n))$ flops with relatively large hidden constant at initialization. The computational and space efficiency of AAP-Hankel is then established when r is small and n is large, and the empirical comparisons in Section 3 confirm our speed advantage. For reader's convenience, a sample MATLAB implementation of AAP-Hankel can be found at

<https://github.com/caesarcai/AAP-Hankel>.

2.3 Recovery Guarantee

The theoretical results of the proposed algorithm are presented in this section while the proofs are presented late in Section 4. We begin with the local convergence guarantee of Algorithm 1, which is provided by the following theorem.

Theorem 2.1 (Local Convergence). *Let $\mathbf{L} = \mathcal{H}(\mathbf{x}) \in \mathbb{C}^{n_1 \times n_2}$ and $\mathbf{s} \in \mathbb{C}^n$ satisfy Assumptions A1 and A2. If the initial guesses \mathbf{L}_0 and \mathbf{s}_0 obey the following conditions:*

$$\|\mathbf{L} - \mathbf{L}_0\|_2 \leq 8\alpha\mu_{c_s}r\sigma_1^L, \quad \|\mathbf{s} - \mathbf{s}_0\|_\infty \leq \frac{\mu_{c_s}r}{n}\sigma_1^L, \quad \text{and} \quad \text{supp}(\mathbf{s}_0) \subset \text{supp}(\mathbf{s}),$$

then the iterates of Algorithm 1 with parameters $\beta = \frac{\mu_{c_s}r}{2n}$ and $\gamma \in (\frac{1}{\sqrt{12}}, 1)$ satisfy

$$\|\mathbf{L} - \mathbf{L}_k\|_2 \leq 8\alpha\mu_{c_s}r\gamma^k\sigma_1^L, \quad \|\mathbf{s} - \mathbf{s}_k\|_\infty \leq \frac{\mu_{c_s}r}{n}\gamma^k\sigma_1^L, \quad \text{and} \quad \text{supp}(\mathbf{s}_k) \subset \text{supp}(\mathbf{s}).$$

As Theorem 2.1 requires a sufficiently close initialization for the local convergence, the following theorem provides the conditions such that the outputs of Algorithm 3 is inside the desired basin of attraction.

Theorem 2.2 (Sufficient Initialization). *Let $\mathbf{L} = \mathcal{H}(\mathbf{x}) \in \mathbb{C}^{n_1 \times n_2}$ and $\mathbf{s} \in \mathbb{C}^n$ satisfy Assumptions A1 and A2. Provided the thresholding parameters $\frac{\mu_{c_s}r\sigma_1^L}{n\sigma_1(\mathcal{H}(\mathbf{z}))} \leq \beta_{init} \leq \frac{3\mu_{c_s}r\sigma_1^L}{n\sigma_1(\mathcal{H}(\mathbf{z}))}$ and $\beta = \frac{\mu_{c_s}r}{2n}$, the outputs of Algorithm 3 satisfy*

$$\|\mathbf{L} - \mathbf{L}_0\|_2 \leq 8\alpha\mu_{c_s}r\sigma_1^L, \quad \|\mathbf{s} - \mathbf{s}_0\|_\infty \leq \frac{\mu_{c_s}r}{n}\sigma_1^L, \quad \text{and} \quad \text{supp}(\mathbf{s}_0) \subset \text{supp}(\mathbf{s}).$$

By the definition of \mathcal{H}^\dagger in (13), it is clear that $\|\mathbf{x} - \mathbf{x}_k\|_2 = \|\mathcal{H}^\dagger(\mathbf{L} - \mathbf{L}_k)\|_2 \leq \|\mathbf{L} - \mathbf{L}_k\|_F \leq \sqrt{2r}\|\mathbf{L} - \mathbf{L}_k\|_2$. Combining Theorem 2.1 with Theorem 2.2, we have established linear convergence of \mathbf{x}_k to \mathbf{x} for AAP-Hankel.

Remark: The theoretical corruption level that can be tolerated by AAP-Hankel is worse than the optimal guarantee $O(1/\mu c_s r)$ obtained in [25]. Here, the looseness of an order in r is caused by replacing spectral norm with Frobenius norm in certain proof steps while we are measuring the convergence errors in teams of spectral norms. Also, the appearance of condition number κ in our requirement is due to the fact that we aim at the fixed rank setting. Nonetheless, empirical results show that AAP-Hankel can indeed tolerate more corruptions in practice, thus the theoretical requirement is highly pessimistic.

2.4 Extension to Multi-Dimensional Signals

For ease of presentation, we focus on the one-dimension signal case in this paper; however, our method is not limited to the signal dimension. In fact, our algorithm and corresponding theoretical results can be easily extended to multi-dimensional cases. For any N -dimensional signals, we can define a Hankel mapping \mathcal{H}_N that maps from a N -dimensional tensor to a N -level Hankel matrix. Due to the space limitation, the definition of \mathcal{H}_N and the corresponding left inverse \mathcal{H}_N^\dagger will be detailed in Supplement A. We emphasize that all the key properties of \mathcal{H} and \mathcal{H}^\dagger are well retained with the properly defined \mathcal{H}_N and \mathcal{H}_N^\dagger . For instance, given a N -dimensional spectrally r -sparse signal \mathbf{X} , one can easily verify that $\mathcal{H}_N(\mathbf{X})$ is rank- r , and the incoherence assumption A1 is still guaranteed for undamped signals with sufficient wrap-around distances between the frequencies. Moreover, for the sparsity assumption A2, $\mathcal{H}_N(\mathbf{S})$ remains the sparsity per row and column provided that \mathbf{S} is sparse. Following the proofs in Section 4, one can trivially extend our theoretical results to the multi-dimensional cases.

3 Numerical Experiments

In this section, we conduct numerical experiments to evaluate the empirical performance of AAP-Hankel. The experiments are executed from MATLAB R2018a on a Windows 10 laptop with Intel i7-8750H CPU (6 cores at 2.2GHz) and 32GB of RAM. We evaluate AAP-Hankel against successful recovery rates and computational efficiency. For the tuning parameter β_{init} and β in our algorithm, we need an estimate of μ . For β_{init} , we also need an estimate of σ_1^L . Empirically, we find one step of Cadzow [35], which costs $O(rn \log(n))$ flops, provides good estimates of those values. Therefore such a routine is included in AAP-Hankel. The truncated SVD in the initialization is computed using the PROPACK package [34]. The relative error at the k^{th} iteration is defined as $err_k = \|\mathbf{z} - \mathbf{x}_k - \mathbf{s}_k\|_2 / \|\mathbf{z}\|_2$. AAP-Hankel is terminated when either err_k is below a threshold tol , or iteration number is greater than 100.

3.1 Empirical Phase Transition

We evaluate the recovery ability of AAP-Hankel and compare it with Robust-EMaC [24], and SAP [25]. Robust-EMaC is implemented using CVX [36] with default parameters. We implement SAP ourselves. The test spectrally sparse signals of length n with r frequency components are formed in the following way: each frequency f_j is randomly generated from $[0, 1)$, and the argument of each complex coefficient a_j is uniformly sampled from $[0, 2\pi)$ while the amplitude is selected to

be $1 + 10^{0.5c_k}$ with c_k being uniformly distributed on $[0, 1]$. We test two different settings for the frequencies: a) no separation condition is imposed on $\{f_k\}_{k=1}^r$, and b) the wrap-around distances between each pair of the randomly drawn frequencies are guaranteed to be greater than $1.5/n$. The locations of the corruptions are chosen uniformly, while the real and imaginary parts of the corruptions are drawn i.i.d. from the uniform distribution over the interval $[-c \cdot \mathbb{E}(|\text{Re}([\mathbf{x}]_i)|), c \cdot \mathbb{E}(|\text{Re}([\mathbf{x}]_i)|)]$ and $[-c \cdot \mathbb{E}(|\text{Im}([\mathbf{x}]_i)|), c \cdot \mathbb{E}(|\text{Im}([\mathbf{x}]_i)|)]$ for some constant $c > 0$, respectively. For a given triple (n, r, α) , 50 random tests are conducted. We consider an algorithm to have successfully reconstructed a test signal if the recovered signal \mathbf{x}_{rec} satisfies $\|\mathbf{x}_{rec} - \mathbf{x}\|_2 / \|\mathbf{x}\|_2 \leq 10^{-3}$. The tests are conducted with $n = 125$ and $c = 1$. An important parameter for both SAP and our algorithm is the target convergence rate γ . For easier problems, a smaller γ can be chosen for computation efficiency. Since we would like the algorithms to have high recovery ability, γ is set to be 0.95 for both algorithms. In Figure 1, we can observe that the two non-convex methods have better performance than the convex method Robust-EMaC, and AAP-Hankel is more favorable compared to SAP when no restriction on frequencies, in terms of recovery rate.

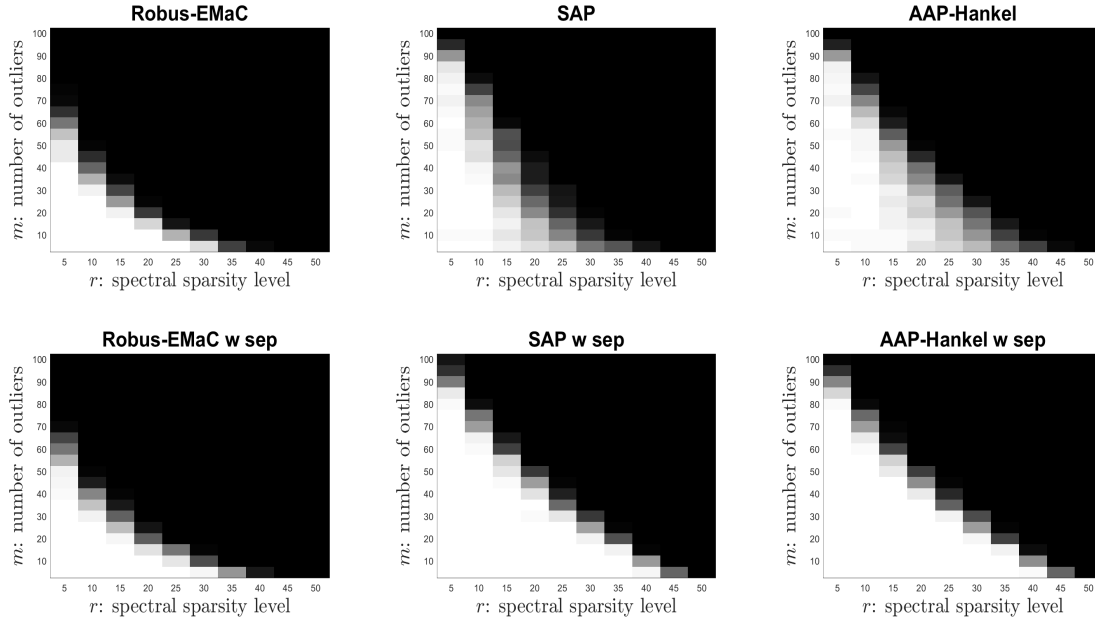


Figure 1: Phase transition comparisons: x -axis is spectral sparsity level r and y -axis is number of corruptions m . Top: no restriction on frequencies of test signals; Bottom: wrap-around distances between frequencies is at least $1.5/n$.

3.2 Computational Efficiency

Next, we compare AAP-Hankel with SAP in terms of computational efficiency. For fair comparisons, we modify SAP such that it does not need to gradually increase the rank. The experiments are conducted on 2D spectrally sparse signals, whose definition can be found in Supplement A. The

tested signals are square matrices with various sizes, generated similarly as in the 1D case without frequency separation. Such sizes are prohibitive for Robust-EMaC, even with a first-order solver. The results reported in Figure 2 are averaged over 10 random tests. The convergence rate parameter is set to $\gamma = 0.5$ for both algorithms. To generate the corruptions, we use $\alpha = 0.1$ as the sparsity parameter, and the magnitude is controlled by $c = 1$. Figure 2 confirms the efficiency of our algorithm. The reported time does not include using Cadzow to estimate μ and σ_1^L since they can be manually tuned by prior knowledge in the real-world applications. Combining the left and middle figures, we can see that the leading complexity of both AAP-Hankel and SAP seem to be $O(rn \log(n))$, depending linearly on n and r , and AAP-Hankel has a smaller constant in the front. The right figure provides empirical evidence for the linear convergence of AAP-Hankel.

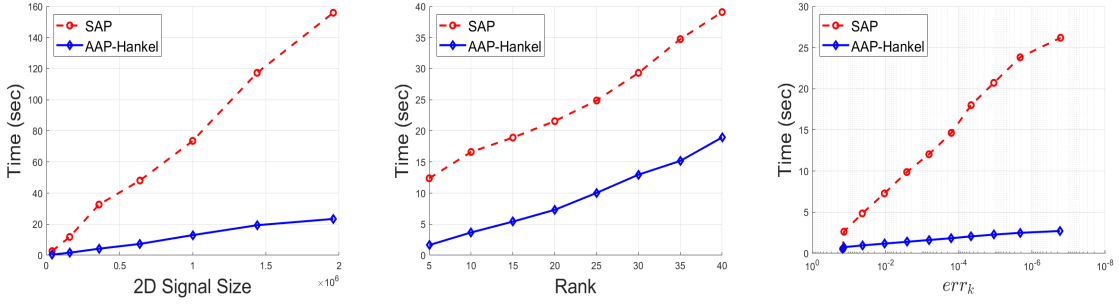


Figure 2: Computational efficiency comparisons. Left: fix rank $r = 5$, runtime plots for 2D signals of size $200^2, 400^2, 600^2, 800^2, 1000^2, 1200^2, 1400^2$; Middle: fix 2D signals size to be 400^2 , runtime plots for rank $r = 5, 10, 15, 20, 25, 30, 35, 40$; Right: fix 2D signals size to be 400^2 and $r = 5$, relative error versus runtime.

3.3 Impulse Corruptions in Nuclear Magnetic Resonance

Our algorithm is applicable to remove impulse corruptions in Nuclear Magnetic Resonance (NMR) spectroscopy signals [6]. The real-world data we are using is a 1D NMR signal of length 32768. Such size is generally prohibited for the convex method Robust-EMaC, even with a first-order solver. In this experiment, we add different amount of sparse outliers to simulate the impulse corruptions caused by malfunctioning sensors, and compare our recovery result to SAP. For different value sets of (α, γ) , we compare the computation time of SAP and AAP-Hankel. We can see from Table 1 that AAP-Hankel is more computational efficient in all 4 settings.

Table 1: Computational time comparisons on the NMR data with different values of (α, γ) .

(α, γ)	(0.2, 0.5)	(0.3, 0.6)	(0.4, 0.7)	(0.5, 0.8)
SAP	39.43 s	59.77 s	77.35 s	124.7 s
AAP-Hankel	16.84 s	22.59 s	24.66 s	32.08 s

The two methods at convergence produce similar results, so we just show a typical recovery result for AAP-Hankel when $\alpha = 0.5$ and $\gamma = 0.8$. In Figure 3, we compare the power spectrum of the impulse corrupted signal, and the result after corruptions removal by AAP-Hankel (reversed for better visualization). We can see from the close-up that the spectral peaks are preserved while the corruptions are removed.

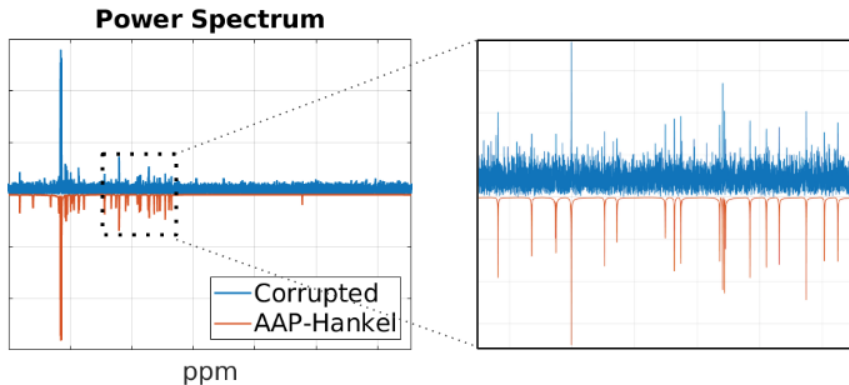


Figure 3: Recovery result of AAP-Hankel on the NMR data.

4 Proofs

In this section, we present the mathematical proofs for the theoretical results in Theorem 2.1 and Theorem 2.2.

4.1 Definitions and Auxiliary Lemmas

We first define some additional notations for the ease of presentation, and then some useful auxiliary lemmas are presented in this subsection.

Definition 4.1. For any vector $\mathbf{z} \in \mathbb{C}^n$, define an augmented Hermitian Hankel mapping $\widehat{\mathcal{H}}$ as

$$\widehat{\mathcal{H}}(\mathbf{z}) = \begin{bmatrix} \mathbf{O} & \mathcal{H}(\mathbf{z}) \\ (\mathcal{H}(\mathbf{z}))^* & \mathbf{O} \end{bmatrix} \in \mathbb{C}^{(n+1) \times (n+1)},$$

where \mathcal{H} is defined as in (4). For any matrix $\mathbf{M} \in \mathbb{C}^{n_1 \times n_2}$, its augmentation is defined using hat symbol, i.e.,

$$\widehat{\mathbf{M}} = \begin{bmatrix} \mathbf{O} & \mathbf{M} \\ \mathbf{M}^* & \mathbf{O} \end{bmatrix}.$$

For subspace projection $\mathcal{P}_{\widetilde{T}_k}$, we also define its augmentation, acting on augmented Hermitian matrix $\widehat{\mathbf{M}}$, as

$$\widehat{\mathcal{P}_{\widetilde{T}_k}}(\widehat{\mathbf{M}}) = \begin{bmatrix} \mathbf{O} & \mathcal{P}_{\widetilde{T}_k}(\mathbf{M}) \\ (\mathcal{P}_{\widetilde{T}_k}(\mathbf{M}))^* & \mathbf{O} \end{bmatrix}. \quad (17)$$

Lemma 4.2. For any $\mathbf{z} \in \mathbb{C}^n$, we have $\|\widehat{\mathcal{H}}(\mathbf{z})\|_\infty = \|\mathcal{H}(\mathbf{z})\|_\infty = \|\mathbf{z}\|_\infty$. Also, for any $\mathbf{M} \in \mathbb{C}^{n_1 \times n_2}$, we have $\|\mathcal{H}^\dagger(\mathbf{M})\|_\infty \leq \|\mathbf{M}\|_\infty$.

Proof. It follows trivially from the definition of $\widehat{\mathcal{H}}$, \mathcal{H} and \mathcal{H}^\dagger . \square

Lemma 4.3. For any $\mathbf{M} \in \mathbb{C}^{n_1 \times n_2}$, consider the Hermitian matrix $\widehat{\mathbf{M}} \in \mathbb{C}^{(n+1) \times (n+1)}$ augmented from \mathbf{M} ,

$$\widehat{\mathbf{M}} = \begin{bmatrix} \mathbf{O} & \mathbf{M} \\ \mathbf{M}^* & \mathbf{O} \end{bmatrix}.$$

Then (1) $\|\widehat{\mathbf{M}}\|_2 = \|\mathbf{M}\|_2$; (2) Suppose the SVD of \mathbf{M} can be written as $\mathbf{P}\Delta\mathbf{Q}^* + \ddot{\mathbf{P}}\ddot{\Delta}\ddot{\mathbf{Q}}^*$, where $\mathbf{P}\Delta\mathbf{Q}^*$ is the best rank- r approximation of \mathbf{M} . Then $\widehat{\mathbf{M}}$ has SVD in the form of $\widehat{\mathbf{P}}\widehat{\Delta}\widehat{\mathbf{Q}}^* + \widehat{\ddot{\mathbf{P}}}\widehat{\ddot{\Delta}}\widehat{\ddot{\mathbf{Q}}}^*$, where

$$\widehat{\mathbf{P}}\widehat{\Delta}\widehat{\mathbf{Q}}^* = \begin{bmatrix} \mathbf{O} & \mathbf{P}\Delta\mathbf{Q}^* \\ \mathbf{Q}\Delta\mathbf{P}^* & \mathbf{O} \end{bmatrix}$$

is the best rank- $2r$ approximations of $\widehat{\mathbf{M}}$; (3) For μ -incoherent \mathbf{L} , its augmentation has SVD $\widehat{\mathbf{L}} = \widehat{\mathbf{U}}\widehat{\Sigma}\widehat{\mathbf{V}}^*$. $\widehat{\mathbf{U}}\widehat{\mathbf{U}}^* = \widehat{\mathbf{V}}\widehat{\mathbf{V}}^*$ and satisfy

$$\max_i \|e_i^T \widehat{\mathbf{U}}\|_2 \leq \sqrt{\frac{\mu c_s r}{n}}, \quad \text{and} \quad \max_j \|e_j^T \widehat{\mathbf{V}}\|_2 \leq \sqrt{\frac{\mu c_s r}{n}}.$$

Proof. It can be verified that

$$\left(\frac{1}{\sqrt{2}} \begin{bmatrix} \mathbf{P} & \ddot{\mathbf{P}} & -\mathbf{P} & -\ddot{\mathbf{P}} \\ \mathbf{Q} & \ddot{\mathbf{Q}} & \mathbf{Q} & \ddot{\mathbf{Q}} \end{bmatrix} \right) \begin{bmatrix} \Delta & & & \\ & \ddot{\Delta} & & \\ & & -\Delta & \\ & & & -\ddot{\Delta} \end{bmatrix} \left(\frac{1}{\sqrt{2}} \begin{bmatrix} \mathbf{P} & \ddot{\mathbf{P}} & -\mathbf{P} & -\ddot{\mathbf{P}} \\ \mathbf{Q} & \ddot{\mathbf{Q}} & \mathbf{Q} & \ddot{\mathbf{Q}} \end{bmatrix} \right)^*$$

is an eigen-decomposition of $\widehat{\mathbf{M}}$. Property (1) is then verified. The best rank- $2r$ approximations of $\widehat{\mathbf{M}}$ can be written as

$$\left(\frac{1}{\sqrt{2}} \begin{bmatrix} \mathbf{P} & -\mathbf{Q} \\ \mathbf{P} & \mathbf{Q} \end{bmatrix} \right) \begin{bmatrix} \Delta & \\ & -\Delta \end{bmatrix} \left(\frac{1}{\sqrt{2}} \begin{bmatrix} \mathbf{P} & -\mathbf{P} \\ \mathbf{Q} & \mathbf{Q} \end{bmatrix} \right)^* = \begin{bmatrix} \mathbf{O} & \mathbf{P}\Delta\mathbf{Q}^* \\ \mathbf{Q}\Delta\mathbf{P}^* & \mathbf{O} \end{bmatrix}. \quad (18)$$

Property (3) follows directly. \square

Lemma 4.4. Let $\mathbf{s} \in \mathbb{C}^n$ be α -sparse. Then it holds that

$$\|\widehat{\mathcal{H}}(\mathbf{s})\|_2 = \|\mathcal{H}(\mathbf{s})\|_2 \leq \alpha n \|\mathbf{s}\|_\infty.$$

Proof. The Hermitian matrix $\widehat{\mathcal{H}}(\mathbf{s})$ has no more than αn nonzero entries per row and column since \mathbf{s} is α -sparse. Then we have

$$\|\mathcal{H}(\mathbf{s})\|_2 = \|\widehat{\mathcal{H}}(\mathbf{s})\|_2 \leq \alpha n \|\widehat{\mathcal{H}}(\mathbf{s})\|_\infty = \alpha n \|\mathbf{s}\|_\infty,$$

where the first equality is by Lemma 4.3, and in the second inequality, we use [10, Lemma 4] for general Hermitian matrices with no more than αn nonzeros entries per row and column. \square

Lemma 4.5. ([11, Lemma 5]) Let Trim be the procedure defined as in Algorithm 2. If $\mathbf{L}_k \in \mathbb{C}^{n_1 \times n_2}$ is a rank- r matrix with

$$\|\mathbf{L}_k - \mathbf{L}\|_2 \leq \frac{\sigma_r^L}{20\sqrt{r}},$$

then the trim output with the level $\sqrt{\frac{\mu c_s r}{n}}$ satisfies

$$\|\tilde{\mathbf{L}}_k - \mathbf{L}\|_F \leq 8\kappa \|\mathbf{L}_k - \mathbf{L}\|_F, \quad (19)$$

$$\max_i \|e_i^T \tilde{\mathbf{U}}_k\|_2 \leq \frac{10}{9} \sqrt{\frac{\mu c_s r}{n}}, \quad \text{and} \quad \max_j \|e_j^T \tilde{\mathbf{V}}_k\|_2 \leq \frac{10}{9} \sqrt{\frac{\mu c_s r}{n}}, \quad (20)$$

where $\tilde{\mathbf{L}}_k = \tilde{\mathbf{U}}_k \tilde{\Sigma}_k \tilde{\mathbf{V}}_k^*$ is the SVD of $\tilde{\mathbf{L}}_k$. Furthermore, it follows that

$$\|\tilde{\mathbf{L}}_k - \mathbf{L}\|_2 \leq 8\sqrt{2r\kappa} \|\mathbf{L}_k - \mathbf{L}\|_2. \quad (21)$$

Lemma 4.6. ([11, Lemma 6]) Let $\mathbf{L} = \mathbf{U}\Sigma\mathbf{V}^*$ and $\tilde{\mathbf{L}}_k = \tilde{\mathbf{U}}_k \tilde{\Sigma}_k \tilde{\mathbf{V}}_k^*$ be the SVD of two rank- r matrices, then

$$\|\mathbf{U}\mathbf{U}^* - \tilde{\mathbf{U}}\tilde{\mathbf{U}}^*\|_2 \leq \frac{\|\tilde{\mathbf{L}}_k - \mathbf{L}\|_2}{\sigma_r^L}, \quad \|\mathbf{V}\mathbf{V}^* - \tilde{\mathbf{V}}\tilde{\mathbf{V}}^*\|_2 \leq \frac{\|\tilde{\mathbf{L}}_k - \mathbf{L}\|_2}{\sigma_r^L}, \quad (22)$$

and

$$\|(\mathcal{I} - \mathcal{P}_{\tilde{T}_k})\mathbf{L}\|_2 \leq \frac{\|\tilde{\mathbf{L}}_k - \mathbf{L}\|_2^2}{\sigma_r^L}. \quad (23)$$

Lemma 4.7. Let $\mathbf{s} \in \mathbb{C}^n$ satisfy Assumption A2. Let $\tilde{\mathbf{L}}_k \in \mathbb{C}^{n_1 \times n_2}$ be a rank- r matrix with $\frac{100}{81}\mu$ -incoherence. That is,

$$\max_i \|e_i^T \tilde{\mathbf{U}}_k\|_2 \leq \frac{10}{9} \sqrt{\frac{\mu c_s r}{n}} \quad \text{and} \quad \max_j \|e_j^T \tilde{\mathbf{V}}_k\|_2 \leq \frac{10}{9} \sqrt{\frac{\mu c_s r}{n}},$$

where $\tilde{\mathbf{L}} = \tilde{\mathbf{U}}_k \tilde{\Sigma}_k \tilde{\mathbf{V}}_k^*$ is the SVD of $\tilde{\mathbf{L}}_k$. If $\text{supp}(\mathbf{s}_k) \subset \Omega$, then

$$\|\mathcal{P}_{\tilde{T}_k} \mathcal{H}(\mathbf{s} - \mathbf{s}_k)\|_\infty \leq 4\alpha \mu c_s r \|\mathbf{s} - \mathbf{s}_k\|_\infty. \quad (24)$$

Proof. By the incoherence assumption of $\tilde{\mathbf{L}}_k$ and the sparsity assumption of $\mathbf{s} - \mathbf{s}_k$, we have

$$\begin{aligned} & [\mathcal{P}_{\tilde{T}_k} \mathcal{H}(\mathbf{s} - \mathbf{s}_k)]_{a,b} \\ &= \langle \mathcal{P}_{\tilde{T}_k} \mathcal{H}(\mathbf{s} - \mathbf{s}_k), \mathbf{e}_a \mathbf{e}_b^T \rangle \\ &= \langle \mathcal{H}(\mathbf{s} - \mathbf{s}_k), \mathcal{P}_{\tilde{T}_k}(\mathbf{e}_a \mathbf{e}_b^T) \rangle \\ &= \langle \mathcal{H}(\mathbf{s} - \mathbf{s}_k), \tilde{\mathbf{U}}_k \tilde{\mathbf{U}}_k^* \mathbf{e}_a \mathbf{e}_b^T + \mathbf{e}_a \mathbf{e}_b^T \tilde{\mathbf{V}}_k \tilde{\mathbf{V}}_k^* - \tilde{\mathbf{U}}_k \tilde{\mathbf{U}}_k^* \mathbf{e}_a \mathbf{e}_b^T \tilde{\mathbf{V}}_k \tilde{\mathbf{V}}_k^* \rangle \\ &= \langle \mathcal{H}(\mathbf{s} - \mathbf{s}_k) \mathbf{e}_b, \tilde{\mathbf{U}}_k \tilde{\mathbf{U}}_k^* \mathbf{e}_a \rangle + \langle \mathbf{e}_a^T \mathcal{H}(\mathbf{s} - \mathbf{s}_k), \mathbf{e}_b^T \tilde{\mathbf{V}}_k \tilde{\mathbf{V}}_k^* \rangle - \langle \mathcal{H}(\mathbf{s} - \mathbf{s}_k), \tilde{\mathbf{U}}_k \tilde{\mathbf{U}}_k^* \mathbf{e}_a \mathbf{e}_b^T \tilde{\mathbf{V}}_k \tilde{\mathbf{V}}_k^* \rangle \\ &\leq \|\mathbf{s} - \mathbf{s}_k\|_\infty \left(\sum_{i|(i,b) \in \Omega} |e_i^T \tilde{\mathbf{U}}_k \tilde{\mathbf{U}}_k^* \mathbf{e}_a| + \sum_{j|(a,j) \in \Omega} |e_b^T \tilde{\mathbf{V}}_k \tilde{\mathbf{V}}_k^* \mathbf{e}_j| \right) \end{aligned}$$

$$\begin{aligned}
& + \|\mathcal{H}(\mathbf{s} - \mathbf{s}_k)\|_2 \|\widetilde{\mathbf{U}}_k \widetilde{\mathbf{U}}_k^* \mathbf{e}_a \mathbf{e}_b^T \widetilde{\mathbf{V}}_k \widetilde{\mathbf{V}}_k^*\|_* \\
& \leq 2\alpha n \frac{100\mu c_s r}{81n} \|\mathbf{s} - \mathbf{s}_k\|_\infty + \alpha n \|\mathbf{s} - \mathbf{s}_k\|_\infty \|\widetilde{\mathbf{U}}_k \widetilde{\mathbf{U}}_k^* \mathbf{e}_a \mathbf{e}_b^T \widetilde{\mathbf{V}}_k \widetilde{\mathbf{V}}_k^*\|_F \\
& \leq \frac{200}{81} \alpha \mu c_s r \|\mathbf{s} - \mathbf{s}_k\|_\infty + \alpha n \|\mathbf{s} - \mathbf{s}_k\|_\infty \frac{100\mu c_s r}{81n} \\
& = \frac{200}{81} \alpha \mu c_s r \|\mathbf{s} - \mathbf{s}_k\|_\infty + \frac{100}{81} \alpha \mu c_s r \|\mathbf{s} - \mathbf{s}_k\|_\infty \\
& \leq 4\alpha \mu c_s r \|\mathbf{s} - \mathbf{s}_k\|_\infty,
\end{aligned}$$

where the first inequality uses Hölder's inequality and the second inequality uses Lemma 4.4. We also use the fact $\widetilde{\mathbf{U}}_k \widetilde{\mathbf{U}}_k^* \mathbf{e}_a \mathbf{e}_b^T \widetilde{\mathbf{V}}_k \widetilde{\mathbf{V}}_k^*$ is a rank-1 matrix to bound its nuclear norm. \square

Lemma 4.8. *Let S be the direct sum of the row space and column space of $\mathbf{M} = \mathbf{P}\mathbf{\Delta}\mathbf{Q}^*$. Then, we have*

$$\|\mathcal{P}_S \mathbf{Z}\|_2 \leq \sqrt{\frac{4}{3}} \|\mathbf{Z}\|_2.$$

Proof. For \mathbf{Z} being Hermitian, this is an extension from the symmetric setting proved in [11, Lemma 8]. For the non-Hermitian \mathbf{Z} , consider the augmented Hermitian matrix $\widehat{\mathbf{Z}}$.

$$\widehat{\mathbf{Z}} = \begin{bmatrix} \mathbf{O} & \mathbf{Z} \\ \mathbf{Z}^* & \mathbf{O} \end{bmatrix}.$$

Denote

$$\widehat{\mathbf{P}} = \frac{1}{\sqrt{2}} \begin{bmatrix} \mathbf{P} & -\mathbf{P} \\ \mathbf{Q} & \mathbf{Q} \end{bmatrix},$$

$$\widehat{\mathbf{P}} \widehat{\mathbf{P}}^* \widehat{\mathbf{Z}} + \widehat{\mathbf{Z}} \widehat{\mathbf{P}} \widehat{\mathbf{P}}^* - \widehat{\mathbf{P}} \widehat{\mathbf{P}}^* \widehat{\mathbf{Z}} \widehat{\mathbf{P}} \widehat{\mathbf{P}}^* = \begin{bmatrix} \mathbf{O} & \mathcal{P}_S \mathbf{Z} \\ (\mathcal{P}_S \mathbf{Z})^* & \mathbf{O} \end{bmatrix}.$$

Apply Lemma 4.3 and the result from Hermitian case,

$$\|\mathcal{P}_S \mathbf{Z}\|_2 = \left\| \begin{bmatrix} \mathbf{O} & \mathcal{P}_S \mathbf{Z} \\ (\mathcal{P}_S \mathbf{Z})^* & \mathbf{O} \end{bmatrix} \right\|_2 \leq \sqrt{\frac{4}{3}} \|\widehat{\mathbf{Z}}\|_2 = \sqrt{\frac{4}{3}} \|\mathbf{Z}\|_2.$$

\square

Lemma 4.9. *Let $\mathbf{W} \in \mathbb{C}^{(n+1) \times r}$ be an orthonormal matrix with μ -incoherence, i.e., $\|\mathbf{e}_i^T \mathbf{W}\|_2 \leq \sqrt{\frac{\mu c_s r}{n}}$ for all i . Then, for any $\widehat{\mathbf{Z}} \in \mathbb{C}^{(n+1) \times (n+1)}$ augmented from a $\mathbf{Z} \in \mathbb{C}^{n_1 \times n_2}$, the inequality*

$$\|\mathbf{e}_i^T \widehat{\mathbf{Z}}^a \mathbf{W}\|_2 \leq \max_l \sqrt{\frac{\mu c_s r}{n}} (\sqrt{n} \|\mathbf{e}_l^T \widehat{\mathbf{Z}}\|_2)^a$$

holds for all i and $a \geq 0$.

Proof. This proof is done by mathematical induction.

Base case: When $a = 0$, $\|\mathbf{e}_i^T \mathbf{W}\|_2 \leq \sqrt{\frac{\mu c_s r}{n}}$ is satisfied following from the assumption.

Induction Hypothesis: $\|e_i^T \widehat{\mathbf{Z}}^a \mathbf{W}\|_2 \leq \max_l \sqrt{\frac{\mu c_s r}{n}} (\sqrt{n} \|e_l^T \widehat{\mathbf{Z}}\|_2)^a$ for all i at the a -th power.

Induction Step: We have

$$\begin{aligned}
\|e_i^T \widehat{\mathbf{Z}}^{a+1} \mathbf{W}\|_2^2 &= \|e_i^T \widehat{\mathbf{Z}} \widehat{\mathbf{Z}}^a \mathbf{W}\|_2^2 \\
&= \sum_j \left| \sum_k [\widehat{\mathbf{Z}}]_{ik} [\widehat{\mathbf{Z}}^a \mathbf{W}]_{kj} \right|^2 \\
&= \sum_{k_1 k_2} \overline{[\widehat{\mathbf{Z}}]_{ik_1}} [\widehat{\mathbf{Z}}]_{ik_2} \sum_j \overline{[\widehat{\mathbf{Z}}^a \mathbf{W}]_{k_1 j}} [\widehat{\mathbf{Z}}^a \mathbf{W}]_{k_2 j} \\
&= \sum_{k_1 k_2} \overline{[\widehat{\mathbf{Z}}]_{ik_1}} [\widehat{\mathbf{Z}}]_{ik_2} \langle e_{k_1}^T \widehat{\mathbf{Z}}^a \mathbf{W}, e_{k_2}^T \widehat{\mathbf{Z}}^a \mathbf{W} \rangle \\
&\leq \sum_{k_1 k_2} |\overline{[\widehat{\mathbf{Z}}]_{ik_1}} [\widehat{\mathbf{Z}}]_{ik_2}| \|e_{k_1}^T \widehat{\mathbf{Z}}^a \mathbf{W}\|_2 \|e_{k_2}^T \widehat{\mathbf{Z}}^a \mathbf{W}\|_2 \\
&\leq \max_l \frac{\mu c_s r}{n} (\sqrt{n} \|e_l^T \widehat{\mathbf{Z}}\|_2)^{2a} \sum_{k_1 k_2} |\overline{[\widehat{\mathbf{Z}}]_{ik_1}} [\widehat{\mathbf{Z}}]_{ik_2}| \\
&\leq \max_l \frac{\mu c_s r}{n} (\sqrt{n} \|e_l^T \widehat{\mathbf{Z}}\|_2)^{2a} (\sqrt{n} \|e_i^T \widehat{\mathbf{Z}}\|_2)^2 \\
&\leq \max_l \frac{\mu c_s r}{n} (\sqrt{n} \|e_l^T \widehat{\mathbf{Z}}\|_2)^{2a+2}.
\end{aligned}$$

The third inequality holds since $\widehat{\mathbf{Z}}$ has no more than n non-zero entries in each row. The proof is then completed by taking a square root from both sides. \square

Lemma 4.10. Let $\mathbf{s} \in \mathbb{C}^n$ satisfy Assumption A2. Let $\mathbf{W} \in \mathbb{C}^{(n+1) \times r}$ be an orthogonal matrix with μ -incoherence, i.e., $\|e_i^T \mathbf{W}\|_2 \leq \sqrt{\frac{\mu c_s r}{n}}$ for all i . Then

$$\|e_i^T (\widehat{\mathcal{H}}(\mathbf{s}))^a \mathbf{W}\|_2 \leq \sqrt{\frac{\mu c_s r}{n}} (\alpha n \|\mathbf{s}\|_\infty)^a$$

for all i and $a \geq 0$.

Proof. This proof is done by mathematical induction.

Base case: When $a = 0$, $\|e_i^T \mathbf{W}\|_2 \leq \sqrt{\frac{\mu c_s r}{n}}$ is satisfied following from the assumption.

Induction Hypothesis: $\|e_i^T (\widehat{\mathcal{H}}(\mathbf{s}))^a \mathbf{W}\|_2 \leq \sqrt{\frac{\mu c_s r}{n}} (\alpha n \|\mathbf{s}\|_\infty)^a$ for all i at the a -th power.

Induction Step: We have

$$\begin{aligned}
\|e_i^T \widehat{\mathcal{H}}(\mathbf{s})^{a+1} \mathbf{W}\|_2^2 &= \|e_i^T \widehat{\mathcal{H}}(\mathbf{s}) \widehat{\mathcal{H}}(\mathbf{s})^a \mathbf{W}\|_2^2 \\
&= \sum_j \left| \sum_k [\widehat{\mathcal{H}}(\mathbf{s})]_{ik} [\widehat{\mathcal{H}}(\mathbf{s})^a \mathbf{W}]_{kj} \right|^2 \\
&= \sum_{k_1 k_2} \overline{[\widehat{\mathcal{H}}(\mathbf{s})]_{ik_1}} [\widehat{\mathcal{H}}(\mathbf{s})]_{ik_2} \sum_j \overline{[\widehat{\mathcal{H}}(\mathbf{s})^a \mathbf{W}]_{k_1 j}} [\widehat{\mathcal{H}}(\mathbf{s})^a \mathbf{W}]_{k_2 j} \\
&= \sum_{k_1 k_2} \overline{[\widehat{\mathcal{H}}(\mathbf{s})]_{ik_1}} [\widehat{\mathcal{H}}(\mathbf{s})]_{ik_2} \langle e_{k_1}^T \widehat{\mathcal{H}}(\mathbf{s})^a \mathbf{W}, e_{k_2}^T \widehat{\mathcal{H}}(\mathbf{s})^a \mathbf{W} \rangle
\end{aligned}$$

$$\begin{aligned}
&\leq \sum_{k_1 k_2} |\overline{[\widehat{\mathcal{H}}(\mathbf{s})]}_{ik_1} [\widehat{\mathcal{H}}(\mathbf{s})]_{ik_2}| \|e_{k_1}^T \widehat{\mathcal{H}}(\mathbf{s})^a \mathbf{W}\|_2 \|e_{k_2}^T \widehat{\mathcal{H}}(\mathbf{s})^a \mathbf{W}\|_2 \\
&\leq \max_l \frac{\mu c_s r}{n} (\alpha n \|\mathbf{s}\|_\infty)^{2a} \sum_{k_1 k_2} |\overline{[\widehat{\mathcal{H}}(\mathbf{s})]}_{ik_1} [\widehat{\mathcal{H}}(\mathbf{s})]_{ik_2}| \\
&\leq \max_l \frac{\mu c_s r}{n} (\alpha n \|\mathbf{s}\|_\infty)^{2a} (\sqrt{\alpha n} \|e_i^T \widehat{\mathcal{H}}(\mathbf{s})\|_2)^2 \\
&\leq \max_l \frac{\mu c_s r}{n} (\alpha n \|\mathbf{s}\|_\infty)^{2a} (\alpha n \|\widehat{\mathcal{H}}(\mathbf{s})\|_\infty)^2 \\
&\leq \max_l \frac{\mu c_s r}{n} (\alpha n \|\mathbf{s}\|_\infty)^{2a+2},
\end{aligned}$$

where the third and fourth inequality uses Assumption A2. The proof is complete by taking a square root from both sides. \square

We use $\tau := 4\alpha\mu c_s r \kappa$ and $v := \tau(48\sqrt{\mu c_s r \kappa} + \mu c_s r)$ in the subsequent proofs.

Lemma 4.11. *Let $\mathbf{L} \in \mathbb{C}^{n_1 \times n_2}$ and $\mathbf{s} \in \mathbb{C}^n$ satisfy Assumptions A1 and A2, respectively. Let $\widetilde{\mathbf{L}}_k \in \mathbb{R}^{n \times n}$ be the trim output of \mathbf{L}_k . If*

$$\|\mathbf{L} - \mathbf{L}_k\|_2 \leq 8\alpha\mu c_s r \gamma^k \sigma_1^L, \quad \|\mathbf{s} - \mathbf{s}_k\|_\infty \leq \frac{\mu c_s r}{n} \gamma^k \sigma_1^L, \text{ and } \text{supp}(\mathbf{s}_k) \subset \Omega,$$

then

$$\|(\mathcal{P}_{\widetilde{T}_k} - \mathcal{I})\mathbf{L} + \mathcal{P}_{\widetilde{T}_k} \mathcal{H}(\mathbf{s} - \mathbf{s}_k)\|_2 \leq \tau \gamma^{k+1} \sigma_r^L, \quad (25)$$

and

$$\max_l \sqrt{n} \|e_l^T [(\mathcal{P}_{\widetilde{T}_k} - \mathcal{I})\mathbf{L} + \mathcal{P}_{\widetilde{T}_k} \mathcal{H}(\mathbf{s} - \mathbf{s}_k)]\|_2 \leq v \gamma^k \sigma_r^L \quad (26)$$

hold for all $k \geq 0$, provided $1 > \gamma \geq 512\tau r \kappa^2 + \frac{1}{\sqrt{12}}$.

Proof. For all $k \geq 0$, we get

$$\begin{aligned}
\|(\mathcal{P}_{\widetilde{T}_k} - \mathcal{I})\mathbf{L} + \mathcal{P}_{\widetilde{T}_k} \mathcal{H}(\mathbf{s} - \mathbf{s}_k)\|_2 &\leq \|(\mathcal{P}_{\widetilde{T}_k} - \mathcal{I})\mathbf{L}\|_2 + \|\mathcal{P}_{\widetilde{T}_k} \mathcal{H}(\mathbf{s} - \mathbf{s}_k)\|_2 \\
&\leq \frac{\|\mathbf{L} - \widetilde{\mathbf{L}}_k\|_2^2}{\sigma_r^L} + \sqrt{\frac{4}{3}} \|\mathcal{H}(\mathbf{s} - \mathbf{s}_k)\|_2 \\
&\leq \frac{(8\sqrt{2}r\kappa)^2 \|\mathbf{L} - \mathbf{L}_k\|_2^2}{\sigma_r^L} + \sqrt{\frac{4}{3}} \alpha n \|\mathbf{s} - \mathbf{s}_k\|_\infty \\
&\leq 128 \cdot 8\alpha\mu c_s r^2 \kappa^3 \|\mathbf{L} - \mathbf{L}_k\|_2 + \sqrt{\frac{4}{3}} \alpha n \|\mathbf{s} - \mathbf{s}_k\|_\infty \\
&\leq \left(512\tau r \kappa^2 + \frac{1}{4} \sqrt{\frac{4}{3}}\right) 4\alpha\mu c_s r \gamma^k \sigma_1^L \\
&\leq 4\alpha\mu c_s r \gamma^{k+1} \sigma_1^L \\
&= \tau \gamma^{k+1} \sigma_r^L
\end{aligned}$$

where the second inequality uses Lemma 4.6 and 4.8, the third inequality uses Lemma 4.4 and 4.5, the fourth inequality follows from the assumption $\frac{\|\mathbf{L} - \mathbf{L}_k\|_2}{\sigma_r^L} \leq 8\alpha\mu c_s r \kappa$, the fifth inequality uses the definition of τ , and the last inequality uses the bound of γ .

To compute the bound of $\max_l \sqrt{n} \|e_l^T [(\mathcal{P}_{\tilde{T}_k} - \mathcal{I})\mathbf{L} + \mathcal{P}_{\tilde{T}_k} \mathcal{H}(\mathbf{s} - \mathbf{s}_k)]\|_2$, first note that

$$\begin{aligned} \max_l \|e_l^T (\mathcal{I} - \mathcal{P}_{\tilde{T}_k})\mathbf{L}\|_2 &= \max_l \|e_l^T (\mathbf{U}\mathbf{U}^* - \tilde{\mathbf{U}}_k \tilde{\mathbf{U}}_k^*) (\mathbf{L} - \tilde{\mathbf{L}}_k) (\mathbf{I} - \tilde{\mathbf{V}}_k \tilde{\mathbf{V}}_k^*)\|_2 \\ &\leq \max_l \|e_l^T (\mathbf{U}\mathbf{U}^* - \tilde{\mathbf{U}}_k \tilde{\mathbf{U}}_k^*)\|_2 \|\mathbf{L} - \tilde{\mathbf{L}}_k\|_2 \|\mathbf{I} - \tilde{\mathbf{V}}_k \tilde{\mathbf{V}}_k^*\|_2 \\ &\leq \left(\frac{19}{9} \sqrt{\frac{\mu c_s r}{n}} \right) \|\mathbf{L} - \tilde{\mathbf{L}}_k\|_2, \end{aligned}$$

where the last inequality follows from the fact \mathbf{L} is μ -incoherent and $\tilde{\mathbf{L}}_k$ is $\frac{100}{81}\mu$ -incoherent. Hence, for all $k \geq 0$, we have

$$\begin{aligned} &\max_l \sqrt{n} \|e_l^T [(\mathcal{P}_{\tilde{T}_k} - \mathcal{I})\mathbf{L} + \mathcal{P}_{\tilde{T}_k} \mathcal{H}(\mathbf{s} - \mathbf{s}_k)]\|_2 \\ &\leq \max_l \sqrt{n} \|e_l^T (\mathcal{I} - \mathcal{P}_{\tilde{T}_k})\mathbf{L}\|_2 + \sqrt{n} \|e_l^T \mathcal{P}_{\tilde{T}_k} \mathcal{H}(\mathbf{s} - \mathbf{s}_k)\|_2 \\ &\leq \frac{19\sqrt{n}}{9} \sqrt{\frac{\mu c_s r}{n}} \|\mathbf{L} - \tilde{\mathbf{L}}_k\|_2 + n \|\mathcal{P}_{\tilde{T}_k} \mathcal{H}(\mathbf{s} - \mathbf{s}_k)\|_\infty \\ &\leq \frac{19}{9} 8\sqrt{2\mu c_s r \kappa} \|\mathbf{L} - \mathbf{L}_k\|_2 + 4n\alpha\mu c_s r \|\mathbf{s} - \mathbf{s}_k\|_\infty \\ &\leq 24\sqrt{\mu c_s r \kappa} \cdot 8\alpha\mu c_s r \gamma^k \sigma_1^L + 4n\alpha\mu c_s r \cdot \frac{\mu c_s r}{n} \gamma^k \sigma_1^L \\ &= v\gamma^k \sigma_r^L, \end{aligned}$$

where the third inequality uses Lemma 4.5 and 4.7. \square

Lemma 4.12. *Let $\mathbf{L} \in \mathbb{C}^{n_1 \times n_2}$ and $\mathbf{s} \in \mathbb{C}^n$ satisfy Assumptions A1 and A2, respectively. Let $\tilde{\mathbf{L}}_k \in \mathbb{C}^{n_1 \times n_2}$ be the trim output of \mathbf{L}_k . For $1 \leq i \leq 2r$, let $\sigma_i^{(k)}$ be the i^{th} singular value of $\mathcal{P}_{\tilde{T}_k} \mathcal{H}(\mathbf{z} - \mathbf{s}_k)$. If*

$$\|\mathbf{L} - \mathbf{L}_k\|_2 \leq 8\alpha\mu c_s r \gamma^k \sigma_1^L, \quad \|\mathbf{s} - \mathbf{s}_k\|_\infty \leq \frac{\mu c_s r}{n} \gamma^k \sigma_1^L, \text{ and } \text{supp}(\mathbf{s}_k) \subset \Omega,$$

then

$$|\sigma_i^L - \sigma_i^{(k)}| \leq \tau \sigma_r^L \quad (27)$$

and

$$(1 - 2\tau)\gamma^j \sigma_1^L \leq \sigma_{r+1}^{(k)} + \gamma^j \sigma_1^{(k)} \leq (1 + 2\tau)\gamma^j \sigma_1^L \quad (28)$$

hold for all $k \geq 0$ and $j \leq k + 1$, provided $1 > \gamma \geq 512\tau r \kappa^2 + \frac{1}{\sqrt{12}}$.

Proof. We have

$$\begin{aligned} \mathcal{P}_{\tilde{T}_k} \mathcal{H}(\mathbf{z} - \mathbf{s}_k) &= \mathcal{P}_{\tilde{T}_k} (\mathbf{L} + \mathcal{H}(\mathbf{s} - \mathbf{s}_k)) \\ &= \mathbf{L} + (\mathcal{P}_{\tilde{T}_k} - \mathcal{I})\mathbf{L} + \mathcal{P}_{\tilde{T}_k} \mathcal{H}(\mathbf{s} - \mathbf{s}_k). \end{aligned}$$

Hence, by Weyl's inequality and (25) in Lemma 4.11, we can see that

$$|\sigma_i^L - \sigma_i^{(k)}| \leq \|(\mathcal{P}_{\tilde{T}_k} - \mathcal{I})\mathbf{L} + \mathcal{P}_{\tilde{T}_k} \mathcal{H}(\mathbf{s} - \mathbf{s}_k)\|_2$$

$$\leq \tau \gamma^{k+1} \sigma_r^L$$

hold for all i and $k \geq 0$. So the first claim is proved since $\gamma < 1$.

Notice that $\sigma_{r+1}^L = 0$, so we have

$$\begin{aligned} |\sigma_{r+1}^{(k)} + \gamma^j \sigma_1^{(k)} - \gamma^j \sigma_1^L| &= |\sigma_{r+1}^{(k)} - \sigma_{r+1}^L + \gamma^j \sigma_1^{(k)} - \gamma^j \sigma_1^L| \\ &\leq \tau \gamma^{k+1} \sigma_r^L + \tau \gamma^{j+k+1} \sigma_r^L \\ &\leq (1 + \gamma^{k+1}) \tau \gamma^j \sigma_r^L \\ &\leq 2\tau \gamma^j \sigma_1^L \end{aligned}$$

for all $j \leq k+1$. This completes the proof of the second claim. \square

4.2 Local Analysis

Overall, the proof of local convergence consists of two steps:

- When $\|\mathbf{L} - \mathbf{L}_k\|_2$ and $\|\mathbf{s} - \mathbf{s}_k\|_\infty$ are sufficiently small, and $\text{supp}(\mathbf{s}_k) \subset \Omega$, then $\|\mathbf{L} - \mathbf{L}_{k+1}\|_2$ decreases in some sense by a constant factor (see Lemma 4.13) and $\|\mathbf{L} - \mathbf{L}_{k+1}\|_\infty$ is small (see Lemma 4.14).
- When $\|\mathbf{L} - \mathbf{L}_{k+1}\|_\infty$ is sufficiently small, we can choose ζ_{k+1} such that $\text{supp}(\mathbf{s}_{k+1}) \subset \Omega$ and $\|\mathbf{s} - \mathbf{s}_{k+1}\|_\infty$ is small (see Lemma 4.15).

These results will be presented in a set of lemmas. Again, we denote $\tau := 4\alpha\mu c_s r \kappa$ and $v := \tau(48\sqrt{\mu c_s r \kappa} + \mu c_s r)$, as we have done in auxiliary lemmas.

Lemma 4.13. *Let $\mathbf{L} \in \mathbb{C}^{n_1 \times n_2}$ and $\mathbf{s} \in \mathbb{C}^n$ satisfy Assumptions A1 and A2, respectively. Let $\tilde{\mathbf{L}}_k \in \mathbb{C}^{n_1 \times n_2}$ be the trim output of \mathbf{L}_k . If*

$$\|\mathbf{L} - \mathbf{L}_k\|_2 \leq 8\alpha\mu c_s r \gamma^k \sigma_1^L, \quad \|\mathbf{s} - \mathbf{s}_k\|_\infty \leq \frac{\mu c_s r}{n} \gamma^k \sigma_1^L, \quad \text{and } \text{supp}(\mathbf{s}_k) \subset \Omega,$$

then we have

$$\|\mathbf{L} - \mathbf{L}_{k+1}\|_2 \leq 8\alpha\mu c_s r \gamma^{k+1} \sigma_1^L,$$

provided $1 > \gamma \geq 512\tau r \kappa^2 + \frac{1}{\sqrt{12}}$.

Proof. A direct calculation yields

$$\begin{aligned} \|\mathbf{L} - \mathbf{L}_{k+1}\|_2 &\leq \|\mathbf{L} - \mathcal{P}_{\tilde{T}_k} \mathcal{H}(\mathbf{z} - \mathbf{s}_k)\|_2 + \|\mathcal{P}_{\tilde{T}_k} \mathcal{H}(\mathbf{z} - \mathbf{s}_k) - \mathbf{L}_{k+1}\|_2 \\ &\leq 2\|\mathbf{L} - \mathcal{P}_{\tilde{T}_k} \mathcal{H}(\mathbf{z} - \mathbf{s}_k)\|_2 \\ &= 2\|\mathbf{L} - \mathcal{P}_{\tilde{T}_k} (\mathbf{L} + \mathcal{H}(\mathbf{s} - \mathbf{s}_k))\|_2 \\ &= 2\|(\mathcal{P}_{\tilde{T}_k} - \mathcal{I})\mathbf{L} + \mathcal{P}_{\tilde{T}_k} \mathcal{H}(\mathbf{s} - \mathbf{s}_k)\|_2 \\ &\leq 2\tau \gamma^{k+1} \sigma_r^L \\ &= 8\alpha\mu c_s r \gamma^{k+1} \sigma_1^L, \end{aligned}$$

where the second inequality follows from the fact $\mathbf{L}_{k+1} = \mathcal{D}_r \mathcal{P}_{\tilde{T}_k} \mathcal{H}(\mathbf{z} - \mathbf{s}_k)$ is the best rank- r approximation of $\mathcal{P}_{\tilde{T}_k} \mathcal{H}(\mathbf{z} - \mathbf{s}_k)$, and the last inequality uses (25) in Lemma 4.11. \square

Lemma 4.14. Let $\mathbf{L} \in \mathbb{C}^{n_1 \times n_2}$ and $\mathbf{s} \in \mathbb{C}^n$ satisfy Assumptions A1 and A2, respectively. Let $\tilde{\mathbf{L}}_k \in \mathbb{C}^{n_1 \times n_2}$ be the trim output of \mathbf{L}_k . If

$$\|\mathbf{L} - \mathbf{L}_k\|_2 \leq 8\alpha\mu c_s r \gamma^k \sigma_1^L, \quad \|\mathbf{s} - \mathbf{s}_k\|_\infty \leq \frac{\mu c_s r}{n} \gamma^k \sigma_1^L, \text{ and } \text{supp}(\mathbf{s}_k) \subset \Omega,$$

then we have

$$\|\mathbf{L} - \mathbf{L}_{k+1}\|_\infty \leq \left(\frac{1}{2} - \tau\right) \frac{\mu c_s r}{n} \gamma^{k+1} \sigma_1^L,$$

provided $1 > \gamma \geq \max\{512\tau r \kappa^2 + \frac{1}{\sqrt{12}}, \frac{2v}{(1-12\tau)(1-\tau-v)^2}\}$ and $\tau < \frac{1}{12}$.

Proof. Consider the augmented matrix of $\mathcal{P}_{\tilde{T}_k} \mathcal{H}(\mathbf{z} - \mathbf{s}_k)$.

$$\widehat{\mathcal{P}}_{\tilde{T}_k} \widehat{\mathcal{H}}(\mathbf{z} - \mathbf{s}_k) = \begin{bmatrix} \mathbf{O} & \mathcal{P}_{\tilde{T}_k} \mathcal{H}(\mathbf{z} - \mathbf{s}_k) \\ (\mathcal{P}_{\tilde{T}_k} \mathcal{H}(\mathbf{z} - \mathbf{s}_k))^* & \mathbf{O} \end{bmatrix} = \widehat{\mathbf{U}}_{k+1} \mathbf{\Lambda} \widehat{\mathbf{U}}_{k+1}^* + \widehat{\mathbf{U}}_{k+1} \mathbf{\Lambda} \widehat{\mathbf{U}}_{k+1}^*$$

where the eigen-decomposition is derived from the SVD of $\mathcal{P}_{\tilde{T}_k} \mathcal{H}(\mathbf{z} - \mathbf{s}_k)$ and $\widehat{\mathbf{U}}_{k+1} \mathbf{\Lambda} \widehat{\mathbf{U}}_{k+1}^*$ is the best rank- $2r$ approximation, as shown in Lemma 4.3. The i^{th} singular values of $\mathcal{P}_{\tilde{T}_k} \mathcal{H}(\mathbf{z} - \mathbf{s}_k)$ are denoted by σ_i instead of $\sigma_i^{(k)}$ for ease of presentation in the proof of this lemma.

Denote $\widehat{\mathbf{Z}} = \widehat{\mathcal{P}}_{\tilde{T}_k} \widehat{\mathcal{H}}(\mathbf{z} - \mathbf{s}_k) - \widehat{\mathbf{L}} = (\widehat{\mathcal{P}}_{\tilde{T}_k} - \mathcal{I}) \widehat{\mathbf{L}} + \widehat{\mathcal{P}}_{\tilde{T}_k} \widehat{\mathcal{H}}(\mathbf{s} - \mathbf{s}_k)$. For $1 \leq j \leq 2r$, let \mathbf{u}_j be the j^{th} eigenvector of $\widehat{\mathbf{U}}_{k+1}$. Noting that $(\widehat{\mathbf{L}} + \widehat{\mathbf{Z}}) \mathbf{u}_j = \lambda_j \mathbf{u}_j$, we have

$$\mathbf{u}_j = \left(\mathbf{I} - \frac{\widehat{\mathbf{Z}}}{\lambda_j}\right)^{-1} \frac{\widehat{\mathbf{L}}}{\lambda_j} \mathbf{u}_j = \left(\mathbf{I} + \frac{\widehat{\mathbf{Z}}}{\lambda_j} + \left(\frac{\widehat{\mathbf{Z}}}{\lambda_j}\right)^2 + \dots\right) \frac{\widehat{\mathbf{L}}}{\lambda_j} \mathbf{u}_j$$

for all \mathbf{u}_j , where the expansion is valid because

$$\frac{\|\widehat{\mathbf{Z}}\|_2}{|\lambda_i|} = \frac{\|\widehat{\mathbf{Z}}\|_2}{|\lambda_{i+r}|} = \frac{\|\mathbf{Z}\|_2}{\sigma_i} \leq \frac{\|\mathbf{Z}\|_2}{\sigma_r} \leq \frac{\tau}{1-\tau} < 1$$

following from (25) in Lemma 4.11 and (27) in Lemma 4.12. This implies

$$\begin{aligned} \widehat{\mathbf{U}}_{k+1} \mathbf{\Lambda} \widehat{\mathbf{U}}_{k+1}^* &= \sum_{j=1}^{2r} \mathbf{u}_j \lambda_j \mathbf{u}_j^* \\ &= \sum_{j=1}^{2r} \left(\sum_{a \geq 0} \left(\frac{\widehat{\mathbf{Z}}}{\lambda_j} \right)^a \frac{\widehat{\mathbf{L}}}{\lambda_j} \right) \mathbf{u}_j \lambda_j \mathbf{u}_j^* \left(\sum_{b \geq 0} \left(\frac{\widehat{\mathbf{Z}}}{\lambda_j} \right)^b \frac{\widehat{\mathbf{L}}}{\lambda_j} \right)^* \\ &= \sum_{a \geq 0} (\widehat{\mathbf{Z}})^a \widehat{\mathbf{L}} \sum_{j=1}^{2r} \left(\mathbf{u}_j \frac{1}{\lambda_j^{a+b+1}} \mathbf{u}_j^* \right) \widehat{\mathbf{L}} \sum_{b \geq 0} (\widehat{\mathbf{Z}})^b \\ &= \sum_{a, b \geq 0} (\widehat{\mathbf{Z}})^a \widehat{\mathbf{L}} \widehat{\mathbf{U}}_{k+1} \mathbf{\Lambda}^{-(a+b+1)} \widehat{\mathbf{U}}_{k+1}^* \widehat{\mathbf{L}} (\widehat{\mathbf{Z}})^b. \end{aligned}$$

From the definition of \mathbf{L}_{k+1} and Lemma 4.3,

$$\widehat{\mathbf{U}}_{k+1} \mathbf{\Lambda} \widehat{\mathbf{U}}_{k+1}^* = \begin{bmatrix} \mathbf{O} & \mathbf{L}_{k+1} \\ \mathbf{L}_{k+1}^* & \mathbf{O} \end{bmatrix}.$$

Thus,

$$\begin{aligned}
& \|\widehat{\mathbf{L}}_{k+1} - \widehat{\mathbf{L}}\|_\infty \\
&= \|\widehat{\mathbf{U}}_{k+1} \mathbf{\Lambda} \widehat{\mathbf{U}}_{k+1}^* - \widehat{\mathbf{L}}\|_\infty \\
&= \|\widehat{\mathbf{L}} \widehat{\mathbf{U}}_{k+1} \mathbf{\Lambda}^{-1} \widehat{\mathbf{U}}_{k+1}^* \widehat{\mathbf{L}} - \widehat{\mathbf{L}} + \sum_{a+b>0} (\widehat{\mathbf{Z}})^a \widehat{\mathbf{L}} \widehat{\mathbf{U}}_{k+1} \mathbf{\Lambda}^{-(a+b+1)} \widehat{\mathbf{U}}_{k+1}^* \widehat{\mathbf{L}} (\widehat{\mathbf{Z}})^b\|_\infty \\
&\leq \|\widehat{\mathbf{L}} \widehat{\mathbf{U}}_{k+1} \mathbf{\Lambda}^{-1} \widehat{\mathbf{U}}_{k+1}^* \widehat{\mathbf{L}} - \widehat{\mathbf{L}}\|_\infty + \sum_{a+b>0} \|(\widehat{\mathbf{Z}})^a \widehat{\mathbf{L}} \widehat{\mathbf{U}}_{k+1} \mathbf{\Lambda}^{-(a+b+1)} \widehat{\mathbf{U}}_{k+1}^* \widehat{\mathbf{L}} (\widehat{\mathbf{Z}})^b\|_\infty \\
&:= \mathbf{Y}_0 + \sum_{a+b>0} \mathbf{Y}_{ab}.
\end{aligned}$$

We will handle \mathbf{Y}_0 first. For each (i, j) entry of \mathbf{Y}_0 , one has

$$\begin{aligned}
\mathbf{Y}_0 &= \max_{ij} |e_i^T (\widehat{\mathbf{L}} \widehat{\mathbf{U}}_{k+1} \mathbf{\Lambda}^{-1} \widehat{\mathbf{U}}_{k+1}^* \widehat{\mathbf{L}} - \widehat{\mathbf{L}}) e_j| \\
&= \max_{ij} |e_i^T \widehat{\mathbf{U}} \widehat{\mathbf{U}}^* (\widehat{\mathbf{L}} \widehat{\mathbf{U}}_{k+1} \mathbf{\Lambda}^{-1} \widehat{\mathbf{U}}_{k+1}^* \widehat{\mathbf{L}} - \widehat{\mathbf{L}}) \widehat{\mathbf{U}} \widehat{\mathbf{U}}^* e_j| \\
&\leq \max_{ij} \|e_i^T \widehat{\mathbf{U}} \widehat{\mathbf{U}}^*\|_2 \|\widehat{\mathbf{L}} \widehat{\mathbf{U}}_{k+1} \mathbf{\Lambda}^{-1} \widehat{\mathbf{U}}_{k+1}^* \widehat{\mathbf{L}} - \widehat{\mathbf{L}}\|_2 \|\widehat{\mathbf{U}} \widehat{\mathbf{U}}^* e_j\|_2 \\
&\leq \frac{\mu_{cs} r}{n} \|\widehat{\mathbf{L}} \widehat{\mathbf{U}}_{k+1} \mathbf{\Lambda}^{-1} \widehat{\mathbf{U}}_{k+1}^* \widehat{\mathbf{L}} - \widehat{\mathbf{L}}\|_2,
\end{aligned}$$

where the second equation follows from the fact $\widehat{\mathbf{L}} = \widehat{\mathbf{U}} \widehat{\mathbf{U}}^* \widehat{\mathbf{L}} = \widehat{\mathbf{L}} \widehat{\mathbf{U}} \widehat{\mathbf{U}}^*$. Since $\widehat{\mathbf{L}} = \widehat{\mathbf{U}}_{k+1} \mathbf{\Lambda} \widehat{\mathbf{U}}_{k+1}^* + \widehat{\mathbf{U}}_{k+1} \ddot{\mathbf{A}} \widehat{\mathbf{U}}_{k+1}^* - \widehat{\mathbf{Z}}$, it holds that

$$\begin{aligned}
& \|\widehat{\mathbf{L}} \widehat{\mathbf{U}}_{k+1} \mathbf{\Lambda}^{-1} \widehat{\mathbf{U}}_{k+1}^* \widehat{\mathbf{L}} - \widehat{\mathbf{L}}\|_2 \\
&= \|(\widehat{\mathbf{U}}_{k+1} \mathbf{\Lambda} \widehat{\mathbf{U}}_{k+1}^* + \widehat{\mathbf{U}}_{k+1} \ddot{\mathbf{A}} \widehat{\mathbf{U}}_{k+1}^* - \widehat{\mathbf{Z}}) \widehat{\mathbf{U}}_{k+1} \mathbf{\Lambda}^{-1} \widehat{\mathbf{U}}_{k+1}^* (\widehat{\mathbf{U}}_{k+1} \mathbf{\Lambda} \widehat{\mathbf{U}}_{k+1}^* + \widehat{\mathbf{U}}_{k+1} \ddot{\mathbf{A}} \widehat{\mathbf{U}}_{k+1}^* - \widehat{\mathbf{Z}}) - \widehat{\mathbf{L}}\|_2 \\
&= \|\widehat{\mathbf{U}}_{k+1} \mathbf{\Lambda} \widehat{\mathbf{U}}_{k+1}^* - \widehat{\mathbf{L}} - \widehat{\mathbf{U}}_{k+1} \widehat{\mathbf{U}}_{k+1}^* \widehat{\mathbf{Z}} - \widehat{\mathbf{Z}} \widehat{\mathbf{U}}_{k+1} \widehat{\mathbf{U}}_{k+1}^* + \widehat{\mathbf{Z}} \widehat{\mathbf{U}}_{k+1} \mathbf{\Lambda}^{-1} \widehat{\mathbf{U}}_{k+1}^* \widehat{\mathbf{Z}}\|_2 \\
&\leq \|\widehat{\mathbf{Z}} - \widehat{\mathbf{U}}_{k+1} \ddot{\mathbf{A}} \widehat{\mathbf{U}}_{k+1}^*\|_2 + 2\|\widehat{\mathbf{Z}}\|_2 + \frac{\|\widehat{\mathbf{Z}}\|_2^2}{\sigma_r} \\
&\leq \|\widehat{\mathbf{U}}_{k+1} \ddot{\mathbf{A}} \widehat{\mathbf{U}}_{k+1}^*\|_2 + 3\|\widehat{\mathbf{Z}}\|_2 + \frac{\|\widehat{\mathbf{Z}}\|_2^2}{\sigma_r} \\
&= \|\widehat{\mathbf{U}}_{k+1} \ddot{\mathbf{A}} \widehat{\mathbf{U}}_{k+1}^*\|_2 + 3\|\mathbf{Z}\|_2 + \frac{\|\mathbf{Z}\|_2^2}{\sigma_r} \\
&\leq \|\widehat{\mathbf{U}}_{k+1} \ddot{\mathbf{A}} \widehat{\mathbf{U}}_{k+1}^*\|_2 + 4\|\mathbf{Z}\|_2 \\
&\leq \sigma_{r+1} + 4\|\mathbf{Z}\|_2 \leq 5\|\mathbf{Z}\|_2 \leq 5\tau\gamma^{k+1}\sigma_1^L,
\end{aligned}$$

where the third inequality follows from $\frac{\|\mathbf{Z}\|_2}{\sigma_r} \leq \frac{\tau}{1-\tau} < 1$ since $\tau < \frac{1}{2}$, the fifth inequality follows from $\sigma_{r+1} \leq \|\mathbf{Z}\|_2$ since \mathbf{L} is a rank- r matrix, the last inequality uses (25) in Lemma 4.11. Thus, we have

$$\mathbf{Y}_0 \leq \frac{\mu_{cs} r}{n} 5\tau\gamma^{k+1}\sigma_1^L. \quad (29)$$

Next, we derive an upper bound for the rest part. Note that

$$\mathbf{Y}_{ab} = \max_{ij} |e_i^T \widehat{\mathbf{Z}}^a \widehat{\mathbf{L}} \widehat{\mathbf{U}}_{k+1} \mathbf{\Lambda}^{-(a+b+1)} \widehat{\mathbf{U}}_{k+1}^* \widehat{\mathbf{L}} \widehat{\mathbf{Z}}^b e_j|$$

$$\begin{aligned}
&= \max_{i,j} |(e_i^T \widehat{\mathbf{Z}}^a \widehat{\mathbf{U}} \widehat{\mathbf{U}}^*) \widehat{\mathbf{L}} \widehat{\mathbf{U}}_{k+1} \mathbf{\Lambda}^{-(a+b+1)} \widehat{\mathbf{U}}_{k+1}^* \widehat{\mathbf{L}} (\widehat{\mathbf{U}} \widehat{\mathbf{U}}^* \widehat{\mathbf{Z}} e_j)| \\
&\leq \max_{i,j} \|e_i^T \widehat{\mathbf{Z}}^a \widehat{\mathbf{U}}\|_2 \|\widehat{\mathbf{L}} \widehat{\mathbf{U}}_{k+1} \mathbf{\Lambda}^{-(a+b+1)} \widehat{\mathbf{U}}_{k+1}^* \widehat{\mathbf{L}}\|_2 \|\widehat{\mathbf{U}}^* \widehat{\mathbf{Z}}^b e_j\|_2 \\
&\leq \max_l \frac{\mu c_s r}{n} (\sqrt{n} \|e_l^T \mathbf{Z}\|_2)^{a+b} \|\widehat{\mathbf{L}} \widehat{\mathbf{U}}_{k+1} \mathbf{\Lambda}^{-(a+b+1)} \widehat{\mathbf{U}}_{k+1}^* \widehat{\mathbf{L}}\|_2,
\end{aligned}$$

where the last inequality uses Lemma 4.9. Using $\widehat{\mathbf{L}} = \widehat{\mathbf{U}}_{k+1} \mathbf{\Lambda} \widehat{\mathbf{U}}_{k+1}^* + \widehat{\mathbf{U}}_{k+1} \ddot{\mathbf{A}} \widehat{\mathbf{U}}_{k+1}^* - \widehat{\mathbf{Z}}$ again,

$$\begin{aligned}
&\|\widehat{\mathbf{L}} \widehat{\mathbf{U}}_{k+1} \mathbf{\Lambda}^{-(a+b+1)} \widehat{\mathbf{U}}_{k+1}^* \widehat{\mathbf{L}}\|_2 \\
&= \|(\widehat{\mathbf{U}}_{k+1} \mathbf{\Lambda} \widehat{\mathbf{U}}_{k+1}^* + \widehat{\mathbf{U}}_{k+1} \ddot{\mathbf{A}} \widehat{\mathbf{U}}_{k+1}^* - \widehat{\mathbf{Z}}) \widehat{\mathbf{U}}_{k+1} \mathbf{\Lambda}^{-(a+b+1)} \widehat{\mathbf{U}}_{k+1}^* \\
&\quad (\widehat{\mathbf{U}}_{k+1} \mathbf{\Lambda} \widehat{\mathbf{U}}_{k+1}^* + \widehat{\mathbf{U}}_{k+1} \ddot{\mathbf{A}} \widehat{\mathbf{U}}_{k+1}^* - \widehat{\mathbf{Z}})\|_2 \\
&= \|\widehat{\mathbf{U}}_{k+1} \mathbf{\Lambda}^{-(a+b-1)} \widehat{\mathbf{U}}_{k+1}^* - \widehat{\mathbf{U}}_{k+1} \mathbf{\Lambda}^{-(a+b)} \widehat{\mathbf{U}}_{k+1}^* \widehat{\mathbf{Z}} - \widehat{\mathbf{Z}} \widehat{\mathbf{U}}_{k+1} \mathbf{\Lambda}^{-(a+b)} \widehat{\mathbf{U}}_{k+1}^* \\
&\quad + \widehat{\mathbf{Z}} \widehat{\mathbf{U}}_{k+1} \mathbf{\Lambda}^{-(a+b+1)} \widehat{\mathbf{U}}_{k+1}^* \widehat{\mathbf{Z}}\|_2 \\
&\leq \sigma_r^{-(a+b-1)} + 2\sigma_r^{-(a+b)} \|\widehat{\mathbf{Z}}\|_2 + \sigma_r^{-(a+b+1)} \|\widehat{\mathbf{Z}}\|_2^2 \\
&= \sigma_r^{-(a+b-1)} \left(1 + \frac{2\|\mathbf{Z}\|_2}{\sigma_r} + \left(\frac{\|\mathbf{Z}\|_2}{\sigma_r} \right)^2 \right) \\
&= \sigma_r^{-(a+b-1)} \left(1 + \frac{\|\mathbf{Z}\|_2}{\sigma_r} \right)^2 \\
&\leq \sigma_r^{-(a+b-1)} \left(\frac{1}{1-\tau} \right)^2 \\
&\leq \left(\frac{1}{1-\tau} \right)^2 ((1-\tau)\sigma_r^L)^{-(a+b-1)},
\end{aligned}$$

where the second inequality follows from $\frac{\|\mathbf{Z}\|_2}{\sigma_r} \leq \frac{\tau}{1-\tau}$, and the last inequality follows from Lemma 4.12. Together with (26) in Lemma 4.11, we have

$$\begin{aligned}
\sum_{a+b>0} \mathbf{Y}_{ab} &\leq \sum_{a+b>0} \frac{\mu c_s r}{n} \left(\frac{1}{1-\tau} \right)^2 v \gamma^k \sigma_r^L \left(\frac{v \gamma^k \sigma_r^L}{(1-\tau) \sigma_r^L} \right)^{a+b-1} \\
&\leq \frac{\mu c_s r}{n} \left(\frac{1}{1-\tau} \right)^2 v \gamma^k \sigma_1^L \sum_{a+b>0} \left(\frac{v}{1-\tau} \right)^{a+b-1} \\
&= \frac{\mu c_s r}{n} \left(\frac{1}{1-\tau} \right)^2 v \gamma^k \sigma_1^L \left(\frac{1}{1-\frac{v}{1-\tau}} \right)^2 \\
&= \frac{\mu c_s r}{n} \left(\frac{1}{1-\tau-v} \right)^2 v \gamma^k \sigma_1^L, \tag{30}
\end{aligned}$$

where $v < 1-\tau$ can be satisfied is α is small enough. Finally, combining (29) and (30) together gives

$$\|\mathbf{L}_{k+1} - \mathbf{L}\|_\infty = \|\widehat{\mathbf{L}}_{k+1} - \widehat{\mathbf{L}}\|_\infty = \mathbf{Y}_0 + \sum_{a+b>0} \mathbf{Y}_{ab}$$

$$\begin{aligned}
&\leq \frac{\mu c_s r}{n} 5\tau \gamma^{k+1} \sigma_1^L + \frac{\mu c_s r}{n} \left(\frac{1}{1-\tau-v} \right)^2 v \gamma^k \sigma_1^L \\
&\leq \left(\frac{1}{2} - \tau \right) \frac{\mu c_s r}{n} \gamma^{k+1} \sigma_1^L,
\end{aligned}$$

where the last inequality follows from $\gamma \geq \frac{2v}{(1-12\tau)(1-\tau-v)^2}$. \square

Lemma 4.15. *Let $\mathbf{L} \in \mathbb{C}^{n_1 \times n_2}$ and $\mathbf{s} \in \mathbb{C}^n$ satisfy Assumptions A1 and A2, respectively. Let $\tilde{\mathbf{L}}_k \in \mathbb{C}^{n_1 \times n_2}$ be the trim output of \mathbf{L}_k . Recall that $\beta = \frac{\mu c_s r}{2n}$. If*

$$\|\mathbf{L} - \mathbf{L}_k\|_2 \leq 8\alpha \mu c_s r \gamma^k \sigma_1^L, \quad \|\mathbf{s} - \mathbf{s}_k\|_\infty \leq \frac{\mu c_s r}{n} \gamma^k \sigma_1^L, \text{ and } \text{supp}(\mathbf{s}_k) \subset \Omega$$

then we have

$$\text{supp}(\mathbf{s}_{k+1}) \subset \Omega \quad \text{and} \quad \|\mathbf{s} - \mathbf{s}_{k+1}\|_\infty \leq \frac{\mu c_s r}{n} \gamma^{k+1} \sigma_1^L,$$

provided $1 > \gamma \geq \max\{\frac{1}{\sqrt{12}}, \frac{2v}{(1-12\tau)(1-\tau-v)^2}\}$ and $\tau < \frac{1}{12}$.

Proof. We first notice that

$$[\mathbf{s}_{k+1}]_t = [\mathcal{T}_{\zeta_{k+1}}(\mathbf{z} - \mathbf{x}_{k+1})]_t = [\mathcal{T}_{\zeta_{k+1}}(\mathbf{s} + \mathbf{x} - \mathbf{x}_{k+1})]_t = \begin{cases} \mathcal{T}_{\zeta_{k+1}}([\mathbf{s} + \mathbf{x} - \mathbf{x}_{k+1}]_t) & t \in \Omega \\ \mathcal{T}_{\zeta_{k+1}}([\mathbf{x} - \mathbf{x}_{k+1}]_t) & t \in \Omega^c \end{cases}.$$

Let $\sigma_i^{(k)}$ denote i -th singular value of $\mathcal{P}_{\tilde{T}_k} \mathcal{H}(\mathbf{z} - \mathbf{s}_k)$. By Lemmas 4.12 and 4.14, we have

$$\begin{aligned}
\|\mathbf{x} - \mathbf{x}_{k+1}\|_\infty &\leq \|\mathbf{L} - \mathbf{L}_{k+1}\|_\infty \\
&\leq \left(\frac{1}{2} - \tau \right) \frac{\mu c_s r}{n} \gamma^{k+1} \sigma_1^L \\
&\leq \left(\frac{1}{2} - \tau \right) \frac{\mu c_s r}{n} \frac{1}{1-2\tau} (\sigma_{r+1}^{(k)} + \gamma^{k+1} \sigma_1^{(k)}) \\
&= \zeta_{k+1}.
\end{aligned}$$

Hence, $[\mathbf{s}_{k+1}]_t = 0$ for all $t \in \Omega^c$, i.e., $\text{supp}(\mathbf{s}_{k+1}) \subset \Omega$. Denote $\Omega_{k+1} := \text{supp}(\mathbf{s}_{k+1}) = \{t \mid |[\mathbf{z} - \mathbf{x}_{k+1}]_t| > \zeta_{k+1}\}$. Then, for any entry of $\mathbf{s} - \mathbf{s}_{k+1}$, it holds that

$$\begin{aligned}
[\mathbf{s} - \mathbf{s}_{k+1}]_t &= \begin{cases} 0 & \\ [\mathbf{x}_{k+1} - \mathbf{x}]_t & \\ [\mathbf{s}]_t & \end{cases} \leq \begin{cases} 0 & \\ \|\mathbf{L} - \mathbf{L}_{k+1}\|_\infty & \\ \|\mathbf{L} - \mathbf{L}_{k+1}\|_\infty + \zeta_{k+1} & \end{cases} \\
&\leq \begin{cases} 0 & (i, j) \in \Omega^c \\ \left(\frac{1}{2} - \tau \right) \frac{\mu c_s r}{n} \gamma^{k+1} \sigma_1^L & (i, j) \in \Omega_{k+1} \\ \frac{\mu c_s r}{n} \gamma^{k+1} \sigma_1^L & (i, j) \in \Omega \setminus \Omega_{k+1}. \end{cases}
\end{aligned}$$

Here the last step follows from Lemma 4.12 which implies $\zeta_{k+1} = \frac{\mu c_s r}{2n} (\sigma_{r+1}^{(k)} + \gamma^{k+1} \sigma_1^{(k)}) \leq \left(\frac{1}{2} - \tau \right) \frac{\mu c_s r}{n} \gamma^{k+1} \sigma_1^L$. Therefore, $\|\mathbf{s} - \mathbf{s}_{k+1}\|_\infty \leq \frac{\mu c_s r}{n} \gamma^{k+1} \sigma_1^L$. \square

Now, we have all the ingredients for the proof of Theorem 2.1, which shows the local linear convergence of Algorithm 1.

Proof of Theorem 2.1. This theorem will be proved by mathematical induction.

Base Case: When $k = 0$, the base case is satisfied by the assumption on the initialization.

Induction Step: Assume we have

$$\|\mathbf{L} - \mathbf{L}_k\|_2 \leq 8\alpha\mu c_s r \gamma^k \sigma_1^L, \quad \|\mathbf{s} - \mathbf{s}_k\|_\infty \leq \frac{\mu c_s r}{n} \gamma^k \sigma_1^L, \quad \text{and} \quad \text{supp}(\mathbf{s}_k) \subset \Omega$$

at the k -th iteration. At the $(k+1)$ -th iteration. It follows directly from Lemmas 4.13 and 4.15 that

$$\|\mathbf{L} - \mathbf{L}_{k+1}\|_2 \leq 8\alpha\mu c_s r \gamma^{k+1} \sigma_1^L, \quad \|\mathbf{s} - \mathbf{s}_{k+1}\|_\infty \leq \frac{\mu c_s r}{n} \gamma^{k+1} \sigma_1^L \quad \text{and} \quad \text{supp}(\mathbf{s}_{k+1}) \subset \Omega,$$

which completes the proof.

Additionally, notice that we overall require $1 > \gamma \geq \max\{512\tau r \kappa^2 + \frac{1}{\sqrt{12}}, \frac{2v}{(1-12\tau)(1-\tau-v)^2}\}$. By the definition of τ and v , one can easily see that the lower bound approaches $\frac{1}{\sqrt{12}}$ when the constant hidden in (7) is sufficiently large. Therefore, the theorem can be proved for any $\gamma \in (\frac{1}{\sqrt{12}}, 1)$. \square

4.3 Initialization

Finally, we show Algorithm 3 provides sufficient initialization for the local convergence.

Proof of Theorem 2.2. The proof can be partitioned into several parts.

Part 1: Note that $\mathbf{L}_{-1} = \mathcal{H}(\mathbf{x}_{-1}) = \mathbf{O}$ and

$$\|\mathbf{L} - \mathbf{L}_{-1}\|_\infty = \|\mathbf{L}\|_\infty = \max_{ij} (\mathbf{e}_i^T \mathbf{U} \mathbf{\Sigma} \mathbf{V}^* \mathbf{e}_j) \leq \max_{ij} \|\mathbf{e}_i^T \mathbf{U}\|_2 \|\mathbf{\Sigma}\|_2 \|\mathbf{V}^* \mathbf{e}_j\|_2 \leq \frac{\mu c_s r}{n} \sigma_1^L,$$

where the last inequality follows from the assumption that \mathbf{L} is μ -incoherent. Thus, with the choice of $\beta_{init} \geq \frac{\mu c_s r \sigma_1^L}{n \sigma_1(\mathcal{H}(\mathbf{z}))}$, we have

$$\|\mathbf{x} - \mathbf{x}_{-1}\|_\infty = \|\mathcal{H}^\dagger(\mathbf{L} - \mathbf{L}_{-1})\|_\infty \leq \|\mathbf{L} - \mathbf{L}_{-1}\|_\infty \leq \beta_{init} \sigma_1(\mathcal{H}(\mathbf{z})) = \zeta_{-1}. \quad (31)$$

Since

$$[\mathbf{s}_{-1}]_t = [\mathcal{T}_{\zeta_{-1}}(\mathbf{z} - \mathbf{x}_{-1})]_t = \begin{cases} \mathcal{T}_{\zeta_{-1}}([\mathbf{s} + \mathbf{x} - \mathbf{x}_{-1}]_t) & t \in \Omega \\ \mathcal{T}_{\zeta_{-1}}([\mathbf{x} - \mathbf{x}_{-1}]_t) & t \in \Omega^c, \end{cases}$$

it follows that $[\mathbf{s}_{-1}]_t = 0$ for all $t \in \Omega^c$, i.e. $\Omega_{-1} := \text{supp}(\mathbf{s}_{-1}) \subset \Omega$. Moreover, for any entry of $\mathbf{s} - \mathbf{s}_{-1}$, we have

$$[\mathbf{s} - \mathbf{s}_{-1}]_t = \begin{cases} 0 \\ [\mathbf{x}_{-1} - \mathbf{x}]_t \\ [\mathbf{s}]_t \end{cases} \leq \begin{cases} 0 \\ \|\mathbf{x} - \mathbf{x}_{-1}\|_\infty \\ \|\mathbf{x} - \mathbf{x}_{-1}\|_\infty + \zeta_{-1} \end{cases} \leq \begin{cases} 0 & t \in \Omega^c \\ \frac{\mu c_s r}{n} \sigma_1^L & t \in \Omega_{-1} \\ \frac{4\mu c_s r}{n} \sigma_1^L & t \in \Omega \setminus \Omega_{-1} \end{cases},$$

where the last inequality follows from $\beta_{init} \leq \frac{3\mu c_s r \sigma_1^L}{n \sigma_1(\mathcal{H}(\mathbf{z}))}$, so that $\zeta_{-1} \leq \frac{3\mu c_s r}{n} \sigma_1^L$. Therefore, it follows that

$$\text{supp}(\mathbf{s}_{-1}) \subset \Omega \quad \text{and} \quad \|\mathbf{s} - \mathbf{s}_{-1}\|_\infty \leq \frac{4\mu c_s r}{n} \sigma_1^L. \quad (32)$$

By Lemma 4.4 and the assumption about the support of \mathbf{s} , we also have

$$\|\mathcal{H}(\mathbf{s} - \mathbf{s}_{-1})\|_2 \leq \alpha n \|\mathbf{s} - \mathbf{s}_{-1}\|_\infty \leq 4\alpha\mu c_s r \sigma_1^L.$$

Part 2: To bound the approximation error of \mathbf{L}_0 to \mathbf{L} in terms of the spectral norm, note that

$$\begin{aligned} \|\mathbf{L} - \mathbf{L}_0\|_2 &= \|\mathcal{H}(\mathbf{x}) - \mathcal{D}_r \mathcal{H}(\mathbf{z} - \mathbf{s}_{-1})\|_2 \\ &\leq 2\|\mathcal{H}(\mathbf{x}) - \mathcal{H}(\mathbf{z} - \mathbf{s}_{-1})\|_2 \\ &= 2\|\mathcal{H}(\mathbf{s} - \mathbf{s}_{-1})\|_2, \end{aligned}$$

where the inequality follows from the fact $\mathbf{L}_0 = \mathcal{D}_r \mathcal{H}(\mathbf{z} - \mathbf{s}_{-1})$ is the best rank r approximation of $\mathcal{H}(\mathbf{z} - \mathbf{s}_{-1})$. It follows immediately that

$$\|\mathbf{L} - \mathbf{L}_0\|_2 \leq 8\alpha\mu c_s r \sigma_1^L. \quad (33)$$

Part 3: We have $\mathcal{H}(\mathbf{z} - \mathbf{s}_{-1}) = \mathbf{L} + \mathcal{H}(\mathbf{s} - \mathbf{s}_{-1})$. Let σ_i denotes the i^{th} singular value of $\mathcal{H}(\mathbf{z} - \mathbf{s}_{-1})$ ordered by $\sigma_1 \geq \sigma_2 \geq \dots$. The application of Weyl's inequality together with the bound of α in Assumption A2 implies that

$$|\sigma_i^L - \sigma_i| \leq \|\mathcal{H}(\mathbf{s} - \mathbf{s}_{-1})\|_2 = \|\widehat{\mathcal{H}}(\mathbf{s} - \mathbf{s}_{-1})\|_2 \leq \frac{\sigma_r^L}{8} \quad (34)$$

holds for all i . Consequently, we have

$$\frac{7}{8}\sigma_i^L \leq \sigma_i \leq \frac{9}{8}\sigma_i^L, \quad \forall 1 \leq i \leq r, \quad (35)$$

$$\frac{\|\mathcal{H}(\mathbf{s} - \mathbf{s}_{-1})\|_2}{\sigma_r} \leq \frac{\frac{\sigma_r^L}{8}}{\frac{7\sigma_r^L}{8}} = \frac{1}{7}. \quad (36)$$

Consider the augmented matrix of $\mathcal{H}(\mathbf{z} - \mathbf{s}_{-1})$,

$$\widehat{\mathcal{H}}(\mathbf{z} - \mathbf{s}_{-1}) = \begin{bmatrix} \mathbf{O} & \mathcal{H}(\mathbf{z} - \mathbf{s}_{-1}) \\ (\mathcal{H}(\mathbf{z} - \mathbf{s}_{-1}))^* & \mathbf{O} \end{bmatrix} = \widehat{\mathbf{U}}_0 \mathbf{\Lambda} \widehat{\mathbf{U}}_0^* + \widehat{\mathbf{U}}_0 \mathbf{\Lambda} \widehat{\mathbf{U}}_0^*$$

where the eigen-decomposition is derived from the SVD of $\mathcal{H}(\mathbf{z} - \mathbf{s}_{-1})$, as shown in Lemma 4.3.

Denote $\mathbf{E} = \mathcal{H}(\mathbf{z} - \mathbf{s}_{-1}) - \mathbf{L} = \mathcal{H}(\mathbf{s} - \mathbf{s}_{-1})$. Then $\widehat{\mathcal{H}}(\mathbf{z} - \mathbf{s}_{-1}) = \widehat{\mathbf{L}} + \widehat{\mathbf{E}}$, where

$$\widehat{\mathbf{L}} = \begin{bmatrix} \mathbf{O} & \mathbf{L} \\ \mathbf{L}^* & \mathbf{O} \end{bmatrix}, \quad \widehat{\mathbf{E}} = \begin{bmatrix} \mathbf{O} & \mathbf{E} \\ \mathbf{E}^* & \mathbf{O} \end{bmatrix}.$$

Let \mathbf{u}_j be the j^{th} column of $\widehat{\mathbf{U}}_0$. We have $(\widehat{\mathbf{L}} + \widehat{\mathbf{E}})\mathbf{u}_j = \lambda_j \mathbf{u}_j$ for $1 \leq j \leq 2r$. We can also derive the following expression

$$\mathbf{u}_j = \left(\mathbf{I} - \frac{\widehat{\mathbf{E}}}{\lambda_j} \right)^{-1} \frac{\widehat{\mathbf{L}}}{\lambda_j} \mathbf{u}_j = \left(\mathbf{I} + \frac{\widehat{\mathbf{E}}}{\lambda_j} + \left(\frac{\widehat{\mathbf{E}}}{\lambda_j} \right)^2 + \dots \right) \frac{\widehat{\mathbf{L}}}{\lambda_j} \mathbf{u}_j$$

for each \mathbf{u}_j , where the expansion in the last equality is valid because $\frac{\|\widehat{\mathbf{E}}\|_2}{|\lambda_i|} = \frac{\|\widehat{\mathbf{E}}\|_2}{|\lambda_{i+r}|} = \frac{\|\mathbf{E}\|_2}{\sigma_i} \leq \frac{1}{7}$ for all $1 \leq i \leq r$ following from (36). This implies

$$\widehat{\mathbf{U}}_0 \mathbf{\Lambda} \widehat{\mathbf{U}}_0^* = \sum_{j=1}^{2r} \mathbf{u}_j \lambda_j \mathbf{u}_j^*$$

$$\begin{aligned}
&= \sum_{j=1}^{2r} \left(\sum_{a \geq 0} \left(\frac{\widehat{\mathbf{E}}}{\lambda_j} \right)^a \frac{\widehat{\mathbf{L}}}{\lambda_j} \right) \mathbf{u}_j \lambda_j \mathbf{u}_j^* \left(\sum_{b \geq 0} \left(\frac{\widehat{\mathbf{E}}}{\lambda_j} \right)^b \frac{\widehat{\mathbf{L}}}{\lambda_j} \right)^* \\
&= \sum_{a \geq 0} (\widehat{\mathbf{E}})^a \widehat{\mathbf{L}} \sum_{j=1}^{2r} \left(\mathbf{u}_j \frac{1}{\lambda_j^{a+b+1}} \mathbf{u}_j^* \right) \widehat{\mathbf{L}} \sum_{b \geq 0} (\widehat{\mathbf{E}})^b \\
&= \sum_{a, b \geq 0} (\widehat{\mathbf{E}})^a \widehat{\mathbf{L}} \widehat{\mathbf{U}}_0 \mathbf{\Lambda}^{-(a+b+1)} \widehat{\mathbf{U}}_0^* \widehat{\mathbf{L}} (\widehat{\mathbf{E}})^b.
\end{aligned}$$

From Lemma 4.3 and the definition of \mathbf{L}_0 , we know that

$$\widehat{\mathbf{U}}_0 \mathbf{\Lambda} \widehat{\mathbf{U}}_0^* = \begin{bmatrix} \mathbf{O} & \mathbf{L}_0 \\ \mathbf{L}_0^* & \mathbf{O} \end{bmatrix}.$$

Therefore,

$$\begin{aligned}
\|\widehat{\mathbf{L}}_0 - \widehat{\mathbf{L}}\|_\infty &= \|\widehat{\mathbf{U}}_0 \mathbf{\Lambda} \widehat{\mathbf{U}}_0^* - \widehat{\mathbf{L}}\|_\infty \\
&= \|\widehat{\mathbf{L}} \widehat{\mathbf{U}}_0 \mathbf{\Lambda}^{-1} \widehat{\mathbf{U}}_0^* \widehat{\mathbf{L}} - \widehat{\mathbf{L}} + \sum_{a+b>0} (\widehat{\mathbf{E}})^a \widehat{\mathbf{L}} \widehat{\mathbf{U}}_0 \mathbf{\Lambda}^{-(a+b+1)} \widehat{\mathbf{U}}_0^* \widehat{\mathbf{L}} (\widehat{\mathbf{E}})^b\|_\infty \\
&\leq \|\widehat{\mathbf{L}} \widehat{\mathbf{U}}_0 \mathbf{\Lambda}^{-1} \widehat{\mathbf{U}}_0^* \widehat{\mathbf{L}} - \widehat{\mathbf{L}}\|_\infty + \sum_{a+b>0} \|(\widehat{\mathbf{E}})^a \widehat{\mathbf{L}} \widehat{\mathbf{U}}_0 \mathbf{\Lambda}^{-(a+b+1)} \widehat{\mathbf{U}}_0^* \widehat{\mathbf{L}} (\widehat{\mathbf{E}})^b\|_\infty \\
&:= \mathbf{Y}_0 + \sum_{a+b>0} \mathbf{Y}_{ab}.
\end{aligned}$$

We will handle \mathbf{Y}_0 first. For each (i, j) entry of \mathbf{Y}_0 , we have

$$\begin{aligned}
\mathbf{Y}_0 &= \max_{ij} |e_i^T (\widehat{\mathbf{L}} \widehat{\mathbf{U}}_0 \mathbf{\Lambda}^{-1} \widehat{\mathbf{U}}_0^* \widehat{\mathbf{L}} - \widehat{\mathbf{L}}) e_j| \\
&= \max_{ij} |e_i^T \widehat{\mathbf{U}} \widehat{\mathbf{U}}^* (\widehat{\mathbf{L}} \widehat{\mathbf{U}}_0 \mathbf{\Lambda}^{-1} \widehat{\mathbf{U}}_0^* \widehat{\mathbf{L}} - \widehat{\mathbf{L}}) \widehat{\mathbf{U}} \widehat{\mathbf{U}}^* e_j| \\
&\leq \max_{ij} \|e_i^T \widehat{\mathbf{U}} \widehat{\mathbf{U}}^*\|_2 \|\widehat{\mathbf{L}} \widehat{\mathbf{U}}_0 \mathbf{\Lambda}^{-1} \widehat{\mathbf{U}}_0^* \widehat{\mathbf{L}} - \widehat{\mathbf{L}}\|_2 \|\widehat{\mathbf{U}} \widehat{\mathbf{U}}^* e_j\|_2 \\
&\leq \frac{\mu c_s r}{n} \|\widehat{\mathbf{L}} \widehat{\mathbf{U}}_0 \mathbf{\Lambda}^{-1} \widehat{\mathbf{U}}_0^* \widehat{\mathbf{L}} - \widehat{\mathbf{L}}\|_2,
\end{aligned}$$

where the second equation follows from the fact $\widehat{\mathbf{L}} = \widehat{\mathbf{U}} \widehat{\mathbf{U}}^* \widehat{\mathbf{L}} = \widehat{\mathbf{L}} \widehat{\mathbf{U}} \widehat{\mathbf{U}}^*$. Since $\widehat{\mathbf{L}} = \widehat{\mathbf{U}}_0 \mathbf{\Lambda} \widehat{\mathbf{U}}_0^* + \widehat{\mathbf{U}}_0 \mathbf{\Lambda} \widehat{\mathbf{U}}_0^* - \widehat{\mathbf{E}}$,

$$\begin{aligned}
&\|\widehat{\mathbf{L}} \widehat{\mathbf{U}}_0 \mathbf{\Lambda}^{-1} \widehat{\mathbf{U}}_0^* \widehat{\mathbf{L}} - \widehat{\mathbf{L}}\|_2 \\
&= \|(\widehat{\mathbf{U}}_0 \mathbf{\Lambda} \widehat{\mathbf{U}}_0^* + \widehat{\mathbf{U}} \mathbf{\Lambda} \widehat{\mathbf{U}}^* - \widehat{\mathbf{E}}) \widehat{\mathbf{U}}_0 \mathbf{\Lambda}^{-1} \widehat{\mathbf{U}}_0^* (\widehat{\mathbf{U}}_0 \mathbf{\Lambda} \widehat{\mathbf{U}}_0^* + \widehat{\mathbf{U}} \mathbf{\Lambda} \widehat{\mathbf{U}}^* - \widehat{\mathbf{E}}) - \widehat{\mathbf{L}}\|_2 \\
&= \|\widehat{\mathbf{U}}_0 \mathbf{\Lambda} \widehat{\mathbf{U}}_0^* - \widehat{\mathbf{L}} - \widehat{\mathbf{U}}_0 \widehat{\mathbf{U}}_0^* \widehat{\mathbf{E}} - \widehat{\mathbf{E}} \widehat{\mathbf{U}}_0 \widehat{\mathbf{U}}_0^* + \widehat{\mathbf{E}} \widehat{\mathbf{U}}_0 \mathbf{\Lambda}^{-1} \widehat{\mathbf{U}}_0^* \widehat{\mathbf{E}}\|_2 \\
&\leq \|\widehat{\mathbf{E}} - \widehat{\mathbf{U}}_0 \mathbf{\Lambda} \widehat{\mathbf{U}}_0^*\|_2 + 2\|\widehat{\mathbf{E}}\|_2 + \frac{\|\widehat{\mathbf{E}}\|_2^2}{\sigma_r} \\
&\leq \|\widehat{\mathbf{U}}_0 \mathbf{\Lambda} \widehat{\mathbf{U}}_0^*\|_2 + 3\|\widehat{\mathbf{E}}\|_2 + \frac{\|\widehat{\mathbf{E}}\|_2^2}{\sigma_r}
\end{aligned}$$

$$\begin{aligned}
&= \|\widehat{\mathbf{U}}_0 \ddot{\mathbf{A}} \widehat{\mathbf{U}}_0^*\|_2 + 3\|\mathbf{E}\|_2 + \frac{\|\mathbf{E}\|_2^2}{\sigma_r} \\
&\leq \|\widehat{\mathbf{U}}_0 \ddot{\mathbf{A}} \widehat{\mathbf{U}}_0^*\|_2 + 4\|\mathbf{E}\|_2 \\
&= \sigma_{r+1} + 4\|\mathbf{E}\|_2 \\
&\leq 5\|\mathbf{E}\|_2,
\end{aligned}$$

where the third inequality follows from (36), and the last from (34), i.e., $\sigma_{r+1} \leq \|\mathbf{E}\|_2$ since $\sigma_{r+1}^L = 0$. Together, we have

$$\mathbf{Y}_0 \leq \frac{5\mu c_s r}{n} \|\mathbf{E}\|_2 \leq 5\alpha\mu c_s r \|\mathbf{E}\|_\infty, \quad (37)$$

where the last inequality follows from Lemma 4.4.

Next, we will find an upper bound for the rest part. Note that

$$\begin{aligned}
\mathbf{Y}_{ab} &= \max_{ij} |e_i^T (\widehat{\mathbf{E}})^a \widehat{\mathbf{L}} \widehat{\mathbf{U}}_0 \mathbf{\Lambda}^{-(a+b+1)} \widehat{\mathbf{U}}_0^* \widehat{\mathbf{L}} (\widehat{\mathbf{E}})^b e_j| \\
&= \max_{ij} |(e_i^T (\widehat{\mathbf{E}})^a \widehat{\mathbf{U}} \widehat{\mathbf{U}}^*) \widehat{\mathbf{L}} \widehat{\mathbf{U}}_0 \mathbf{\Lambda}^{-(a+b+1)} \widehat{\mathbf{U}}_0^* \widehat{\mathbf{L}} (\widehat{\mathbf{U}} \widehat{\mathbf{U}}^* (\widehat{\mathbf{E}}^*)^b e_j)| \\
&\leq \max_{ij} \|e_i^T (\widehat{\mathbf{E}})^a \widehat{\mathbf{U}}\|_2 \|\widehat{\mathbf{L}} \widehat{\mathbf{U}}_0 \mathbf{\Lambda}^{-(a+b+1)} \widehat{\mathbf{U}}_0^* \widehat{\mathbf{L}}\|_2 \|\widehat{\mathbf{U}}^* (\widehat{\mathbf{E}}^*)^b e_j\|_2 \\
&\leq \frac{\mu c_s r}{n} (\alpha n \|\widehat{\mathbf{E}}\|_\infty)^{a+b} \|\widehat{\mathbf{L}} \widehat{\mathbf{U}}_0 \mathbf{\Lambda}^{-(a+b+1)} \widehat{\mathbf{U}}_0^* \widehat{\mathbf{L}}\|_2 \\
&= (\alpha\mu c_s r \|\mathbf{E}\|_\infty) (\alpha n \|\mathbf{E}\|_\infty)^{a+b-1} \|\widehat{\mathbf{L}} \widehat{\mathbf{U}}_0 \mathbf{\Lambda}^{-(a+b+1)} \widehat{\mathbf{U}}_0^* \widehat{\mathbf{L}}\|_2 \\
&\leq \alpha\mu c_s r \|\mathbf{E}\|_\infty \left(\frac{\sigma_r^L}{8}\right)^{a+b-1} \|\widehat{\mathbf{L}} \widehat{\mathbf{U}}_0 \mathbf{\Lambda}^{-(a+b+1)} \widehat{\mathbf{U}}_0^* \widehat{\mathbf{L}}\|_2
\end{aligned}$$

where the second inequality uses Lemma 4.10. Furthermore, by using $\widehat{\mathbf{L}} = \widehat{\mathbf{U}}_0 \mathbf{\Lambda} \widehat{\mathbf{U}}_0^* + \widehat{\mathbf{U}}_0 \ddot{\mathbf{A}} \widehat{\mathbf{U}}_0^* - \widehat{\mathbf{E}}$ again, we have

$$\begin{aligned}
&\|\widehat{\mathbf{L}} \widehat{\mathbf{U}}_0 \mathbf{\Lambda}^{-(a+b+1)} \widehat{\mathbf{U}}_0^* \widehat{\mathbf{L}}\|_2 \\
&= \|(\widehat{\mathbf{U}}_0 \mathbf{\Lambda} \widehat{\mathbf{U}}_0^* + \widehat{\mathbf{U}}_0 \ddot{\mathbf{A}} \widehat{\mathbf{U}}_0^* - \widehat{\mathbf{E}}) \widehat{\mathbf{U}}_0 \mathbf{\Lambda}^{-(a+b+1)} \widehat{\mathbf{U}}_0^* (\widehat{\mathbf{U}}_0 \mathbf{\Lambda} \widehat{\mathbf{U}}_0^* + \widehat{\mathbf{U}}_0 \ddot{\mathbf{A}} \widehat{\mathbf{U}}_0^* - \widehat{\mathbf{E}})\|_2 \\
&= \|\widehat{\mathbf{U}}_0 \mathbf{\Lambda}^{-(a+b-1)} \widehat{\mathbf{U}}_0^* - \widehat{\mathbf{U}}_0 \mathbf{\Lambda}^{-(a+b)} \widehat{\mathbf{U}}_0^* \widehat{\mathbf{E}} - \widehat{\mathbf{E}} \widehat{\mathbf{U}}_0 \mathbf{\Lambda}^{-(a+b)} \widehat{\mathbf{U}}_0^* + \widehat{\mathbf{E}} \widehat{\mathbf{U}}_0 \mathbf{\Lambda}^{-(a+b+1)} \widehat{\mathbf{U}}_0^* \widehat{\mathbf{E}}\|_2 \\
&\leq \sigma_r^{-(a+b-1)} + \sigma_r^{-(a+b)} \|\widehat{\mathbf{E}}\|_2 + \sigma_r^{-(a+b)} \|\widehat{\mathbf{E}}\|_2 + \sigma_r^{-(a+b+1)} \|\widehat{\mathbf{E}}\|_2^2 \\
&= \sigma_r^{-(a+b-1)} \left(1 + \frac{2\|\mathbf{E}\|_2}{\sigma_r} + \left(\frac{\|\mathbf{E}\|_2}{\sigma_r}\right)^2\right) \\
&= \sigma_r^{-(a+b-1)} \left(1 + \frac{\|\mathbf{E}\|_2}{\sigma_r}\right)^2 \\
&\leq 2\sigma_r^{-(a+b-1)} \\
&\leq 2\left(\frac{7}{8}\sigma_r^L\right)^{-(a+b-1)},
\end{aligned}$$

where the second inequality follows from (36) and the last inequality follows from (35). Together,

we have

$$\begin{aligned}
\sum_{a+b>0} \mathbf{Y}_{ab} &\leq \sum_{a+b>0} 2\alpha\mu c_s r \|\mathbf{E}\|_\infty \left(\frac{\frac{1}{8}\sigma_r^L}{\frac{7}{8}\sigma_r^L} \right)^{a+b-1} \\
&\leq 2\alpha\mu c_s r \|\mathbf{E}\|_\infty \sum_{a+b>0} \left(\frac{1}{7} \right)^{a+b-1} \\
&= 2\alpha\mu c_s r \|\mathbf{E}\|_\infty \left(\frac{1}{1-\frac{1}{7}} \right)^2 \\
&\leq 3\alpha\mu c_s r \|\mathbf{E}\|_\infty.
\end{aligned} \tag{38}$$

Finally, combining (37) and (38) together yields

$$\begin{aligned}
\|\mathbf{L}_0 - \mathbf{L}\|_\infty &= \|\widehat{\mathbf{L}}_0 - \widehat{\mathbf{L}}\|_\infty = \mathbf{Y}_0 + \sum_{a+b>0} \mathbf{Y}_{ab} \\
&\leq 5\alpha\mu c_s r \|\mathbf{E}\|_\infty + 3\alpha\mu c_s r \|\mathbf{E}\|_\infty \\
&\leq \frac{\mu c_s r}{4n} \sigma_1^L,
\end{aligned} \tag{39}$$

where the last step uses (32) and the bound of α in Assumption A2.

Part 4: From the thresholding rule, we know that

$$[\mathbf{s}_0]_t = [\mathcal{T}_{\zeta_0}(\mathbf{z} - \mathbf{x}_0)]_t = \begin{cases} \mathcal{T}_{\zeta_0}([\mathbf{s} + \mathbf{x} - \mathbf{x}_0]_t) & t \in \Omega \\ \mathcal{T}_{\zeta_0}([\mathbf{x} - \mathbf{x}_0]_t) & t \in \Omega^c \end{cases}.$$

So (35), (39) and $\zeta_0 = \frac{\mu c_s r}{2n} \sigma_1$ imply $[\mathbf{s}_0]_t = 0$ for all $t \in \Omega^c$, i.e., $\text{supp}(\mathbf{s}_0) := \Omega_0 \subset \Omega$. Also, for any entry of $(\mathbf{s} - \mathbf{s}_0)$, it holds that

$$[\mathbf{s} - \mathbf{s}_0]_t = \begin{cases} 0 \\ [\mathbf{x}_0 - \mathbf{x}]_t \\ [\mathbf{s}]_t \end{cases} \leq \begin{cases} 0 \\ \|\mathbf{L} - \mathbf{L}_0\|_\infty \\ \|\mathbf{L} - \mathbf{L}_0\|_\infty + \zeta_0 \end{cases} \leq \begin{cases} 0 & t \in \Omega^c \\ \frac{\mu c_s r}{4n} \sigma_1^L & t \in \Omega_0 \\ \frac{\mu c_s r}{n} \sigma_1^L & t \in \Omega \setminus \Omega_0. \end{cases}$$

Here the last inequality follows from (35) which implies $\zeta_0 = \frac{\mu c_s r}{2n} \sigma_1 \leq \frac{3\mu c_s r}{4n} \sigma_1^L$. Therefore, we have

$$\text{supp}(\mathbf{s}_0) \subset \Omega \quad \text{and} \quad \|\mathbf{s} - \mathbf{s}_0\|_\infty \leq \frac{\mu c_s r}{n} \sigma_1^L.$$

The proof is complete by noting (33) and the above results. \square

5 Conclusion

In this paper, we propose a highly efficient non-convex algorithm, dubbed AAP-Hankel, to solve the robust low-rank Hankel matrix reconstruction problem, and its application on spectrally sparse signals. Guaranteed exact recovery with a linear convergence rate has been established for AAP-Hankel. Numerical experiments, compared with convex and non-convex methods in the literature, confirm its computational efficiency and robustness to corruptions. The experiments also suggest the

derived tolerance of corruptions is highly pessimistic, and one possible further direction is to improve the theoretical analysis. It would also be interesting to consider noisy measurements together with sparse corruptions. We empirically observe that the proposed algorithm is also robust to additive noise, and always find a rank- r Hankel matrix at convergence. Another further research direction is to extend the algorithm and analysis to the missing data case.

References

- [1] Liliana Borcea, George Papanicolaou, Chrysoula Tsogka, and James Berryman. Imaging and time reversal in random media. *Inverse Problems*, 18(5):1247, 2002.
- [2] Joel A Tropp, Jason N Laska, Marco F Duarte, Justin K Romberg, and Richard G Baraniuk. Beyond Nyquist: Efficient sampling of sparse bandlimited signals. *arXiv preprint arXiv:0902.0026*, 2009.
- [3] Deborah Cohen, Shahar Tsiper, and Yonina C Eldar. Analog-to-digital cognitive radio: Sampling, detection, and hardware. *IEEE Signal Processing Magazine*, 35(1):137–166, 2018.
- [4] Ye Li, Javad Razavilar, and KJ Ray Liu. A high-resolution technique for multidimensional NMR spectroscopy. *IEEE Transactions on Biomedical Engineering*, 45(1):78–86, 1998.
- [5] Daniel J Holland, Mark J Bostock, Lynn F Gladden, and Daniel Nietlispach. Fast multidimensional NMR spectroscopy using compressed sensing. *Angewandte Chemie International Edition*, 50(29):6548–6551, 2011.
- [6] Xiaobo Qu, Maxim Mayzel, Jian-Feng Cai, Zhong Chen, and Vladislav Orekhov. Accelerated NMR spectroscopy with low-rank reconstruction. *Angewandte Chemie International Edition*, 54(3):852–854, 2015.
- [7] Lothar Schermelleh, Rainer Heintzmann, and Heinrich Leonhardt. A guide to super-resolution fluorescence microscopy. *The Journal of cell biology*, 190(2):165–175, 2010.
- [8] Yuanxin Xi and David M Rocke. Baseline correction for NMR spectroscopic metabolomics data analysis. *BMC bioinformatics*, 9(1):324, 2008.
- [9] John Wright, Arvind Ganesh, Shankar Rao, Yigang Peng, and Yi Ma. Robust principal component analysis: Exact recovery of corrupted low-rank matrices via convex optimization. In *Advances in neural information processing systems*, pages 2080–2088, 2009.
- [10] Praneeth Netrapalli, UN Niranjan, Sujay Sanghavi, Animashree Anandkumar, and Prateek Jain. Non-convex robust PCA. In *Advances in Neural Information Processing Systems*, pages 1107–1115, 2014.
- [11] HanQin Cai, Jian-Feng Cai, and Ke Wei. Accelerated alternating projections for robust principal component analysis. *Journal of Machine Learning Research*, 20(20):1–33, 2019.
- [12] Hien M Nguyen, Xi Peng, Minh N Do, and Zhi-Pei Liang. Denoising MR spectroscopic imaging data with low-rank approximations. *IEEE Transactions on Biomedical Engineering*, 60(1):78–89, 2013.
- [13] Justin P Haldar. Low-rank modeling of local k -space neighborhoods (LORAKS) for constrained MRI. *IEEE transactions on medical imaging*, 33(3):668–681, 2014.

- [14] Kyong Hwan Jin, Dongwook Lee, and Jong Chul Ye. A general framework for compressed sensing and parallel MRI using annihilating filter based low-rank Hankel matrix. *IEEE Transactions on Computational Imaging*, 2(4):480–495, 2016.
- [15] Parikshit Shah, Badri Narayan Bhaskar, Gongguo Tang, and Benjamin Recht. Linear system identification via atomic norm regularization. In *2012 IEEE 51st IEEE Conference on Decision and Control (CDC)*, pages 6265–6270. IEEE, 2012.
- [16] Maryam Fazel, Ting Kei Pong, Defeng Sun, and Paul Tseng. Hankel matrix rank minimization with applications to system identification and realization. *SIAM Journal on Matrix Analysis and Applications*, 34(3):946–977, 2013.
- [17] Sun-Yuan Kung, K Si Arun, and DV Bhaskar Rao. State-space and singular-value decomposition-based approximation methods for the harmonic retrieval problem. *JOSA*, 73(12):1799–1811, 1983.
- [18] Hirotugu Akaike. Markovian representation of stochastic processes and its application to the analysis of autoregressive moving average processes. In *Selected Papers of Hirotugu Akaike*, pages 223–247. Springer, 1998.
- [19] Kyong Hwan Jin, Ji-Yong Um, Dongwook Lee, Juyoung Lee, Sung-Hong Park, and Jong Chul Ye. MRI artifact correction using sparse + low-rank decomposition of annihilating filter-based Hankel matrix. *Magnetic resonance in medicine*, 78(1):327–340, 2017.
- [20] Wenjing Liao and Albert Fannjiang. MUSIC for single-snapshot spectral estimation: Stability and super-resolution. *Applied and Computational Harmonic Analysis*, 40(1):33–67, 2016.
- [21] Xiaodong Li. Compressed sensing and matrix completion with constant proportion of corruptions. *Constructive Approximation*, 37(1):73–99, 2013.
- [22] Yuejie Chi, Louis L Scharf, Ali Pezeshki, and A Robert Calderbank. Sensitivity to basis mismatch in compressed sensing. *IEEE Transactions on Signal Processing*, 59(5):2182–2195, 2011.
- [23] Carlos Fernandez-Granda, Gongguo Tang, Xiaodong Wang, and Le Zheng. Demixing sines and spikes: Robust spectral super-resolution in the presence of outliers. *Information and Inference: A Journal of the IMA*, 7(1):105–168, 2017.
- [24] Yuxin Chen and Yuejie Chi. Robust spectral compressed sensing via structured matrix completion. *IEEE Transactions on Information Theory*, 60(10):6576–6601, 2014.
- [25] Shuai Zhang and Meng Wang. Correction of simultaneous bad measurements by exploiting the low-rank Hankel structure. In *2018 IEEE International Symposium on Information Theory (ISIT)*, pages 646–650. IEEE, 2018.
- [26] Bart Vandereycken. Low-rank matrix completion by Riemannian optimization. *SIAM Journal on Optimization*, 23(2):1214–1236, 2013.
- [27] P-A Absil, Robert Mahony, and Rodolphe Sepulchre. *Optimization algorithms on matrix manifolds*. Princeton University Press, 2009.
- [28] Benjamin Recht. A simpler approach to matrix completion. *Journal of Machine Learning Research*, 12(Dec):3413–3430, 2011.
- [29] Thanh Ngo and Yousef Saad. Scaled gradients on Grassmann manifolds for matrix completion. In *Advances in Neural Information Processing Systems*, pages 1412–1420, 2012.

- [30] Bamdev Mishra, Gilles Meyer, Silvére Bonnabel, and Rodolphe Sepulchre. Fixed-rank matrix factorizations and Riemannian low-rank optimization. *Computational Statistics*, 29(3-4):591–621, 2014.
- [31] Ke Wei, Jian-Feng Cai, Tony F Chan, and Shingyu Leung. Guarantees of Riemannian optimization for low rank matrix recovery. *SIAM Journal on Matrix Analysis and Applications*, 37(3):1198–1222, 2016.
- [32] Jian-Feng Cai, Tianming Wang, and Ke Wei. Fast and provable algorithms for spectrally sparse signal reconstruction via low-rank Hankel matrix completion. *Applied and Computational Harmonic Analysis*, 46(1):94–121, 2019.
- [33] Ling Lu, Wei Xu, and Sanzheng Qiao. A fast SVD for multilevel block Hankel matrices with minimal memory storage. *Numerical Algorithms*, 69(4):875–891, 2015.
- [34] RM Larsen. PROPACK: A software package for the symmetric eigenvalue problem and singular value problems on Lanczos and Lanczos bidiagonalization with partial reorthogonalization, SCCM. URL <http://soi.stanford.edu/rmunk/PROPACK>, 111, 2004.
- [35] James A Cadzow. Signal enhancement-a composite property mapping algorithm. *IEEE Transactions on Acoustics, Speech, and Signal Processing*, 36(1):49–62, 1988.
- [36] Michael Grant and Stephen Boyd. CVX: Matlab software for disciplined convex programming.

AAP-Hankel: Supplemental Materials

A Mapping to Multi-Level Hankel Matrix

As mentioned in subsection 2.4, for N -dimensional spectrally sparse signals, we can construction N -level Hankel mapping, denoted by \mathcal{H}_N . Without loss of generality, we discuss the two-dimensional setting in this section but emphasize that the situation in general N -dimensions is similar. Let $w_j = e^{2\pi i f_{1j} - \tau_{1j}}$ and $z_j = e^{2\pi i f_{2j} - \tau_{2j}}$, where $\{(f_{1j}, f_{2j})\} \in [0, 1]^2$ are pairs of frequencies and $\{(\tau_{1j}, \tau_{2j})\} \in \mathbb{R}_+^2$ are pairs of damping factors. A discrete two-dimensional spectrally r -sparse array $\mathbf{X} \in \mathbb{C}^{N_1 \times N_2}$ can be expressed as

$$[\mathbf{X}]_{c,d} = \sum_{j=1}^r a_j w_j^c z_j^d, \quad (c, d) \in [N_1] \times [N_2],$$

where $\{a_j\} \in \mathbb{C}$ are non-zero complex amplitudes. The mapping to two-level Hankel matrix of \mathbf{X} is given by

$$\mathcal{H}_2(\mathbf{X}) = \begin{bmatrix} \mathcal{H}([\mathbf{X}]_{:,0}) & \mathcal{H}([\mathbf{X}]_{:,1}) & \mathcal{H}([\mathbf{X}]_{:,2}) & \cdots & \cdots & \mathcal{H}([\mathbf{X}]_{:,N_2-n_2}) \\ \mathcal{H}([\mathbf{X}]_{:,1}) & \mathcal{H}([\mathbf{X}]_{:,2}) & \cdots & \cdots & \cdots & \mathcal{H}([\mathbf{X}]_{:,N_2-n_2+1}) \\ \mathcal{H}([\mathbf{X}]_{:,2}) & \cdots & \cdots & \cdots & \cdots & \mathcal{H}([\mathbf{X}]_{:,N_2-n_2+2}) \\ \vdots & \vdots & \vdots & \vdots & \vdots & \vdots \\ \mathcal{H}([\mathbf{X}]_{:,n_2-1}) & \mathcal{H}([\mathbf{X}]_{:,n_2}) & \cdots & \cdots & \cdots & \mathcal{H}([\mathbf{X}]_{:,N_2-1}) \end{bmatrix}, \quad (40)$$

where \mathcal{H} is defined as in (4); that is, each block in $\mathcal{H}_2(\mathbf{X})$ is an $n_1 \times (N_1 - n_1 + 1)$ Hankel matrix corresponding to a column of \mathbf{X} .

Clearly, $\mathcal{H}_2(\mathbf{X})$ is an $(n_1 n_2) \times (N_1 - n_1 + 1)(N_2 - n_2 + 1)$ matrix, where again we want $\mathcal{H}_2(\mathbf{X})$ to be near square, i.e., choose n_1 and n_2 such that $n_1 n_2 \approx (N_1 - n_1 + 1)(N_2 - n_2 + 1)$. Let $c = c_1 + c_2 \cdot n_1$ and $d = d_1 + d_2 \cdot (N_1 - n_1 + 1)$. The $(c, d)^{th}$ entry of $\mathcal{H}_2(\mathbf{X})$ is then given by

$$[\mathcal{H}_2(\mathbf{X})]_{c,d} = [\mathbf{X}]_{c_1+d_1, c_2+d_2} = \sum_{j=1}^r a_j (w_j^{c_1} z_j^{c_2}) (w_j^{d_1} z_j^{d_2}). \quad (41)$$

For each $j \in \{1, \dots, r\}$, we define four vectors $\mathbf{w}_j^{[n_1]}$, $\mathbf{w}_j^{[N_1-n_1+1]}$, $\mathbf{z}_j^{[n_2]}$, and $\mathbf{z}_j^{[N_2-n_2+1]}$ as

$$\mathbf{w}_j^{[n_1]} = \begin{bmatrix} 1 \\ w_j \\ \vdots \\ w_j^{n_1-1} \end{bmatrix}, \mathbf{w}_j^{[N_1-n_1+1]} = \begin{bmatrix} 1 \\ w_j \\ \vdots \\ w_j^{N_1-n_1} \end{bmatrix}, \mathbf{z}_j^{[n_2]} = \begin{bmatrix} 1 \\ z_j \\ \vdots \\ z_j^{n_2-1} \end{bmatrix}, \text{ and } \mathbf{z}_j^{[N_2-n_2+1]} = \begin{bmatrix} 1 \\ z_j \\ \vdots \\ z_j^{N_2-n_2} \end{bmatrix},$$

respectively. Let \mathbf{E}_L be an $(n_1 n_2) \times r$ matrix, where its j^{th} column equals $\mathbf{z}_j^{[n_2]} \otimes \mathbf{w}_j^{[n_1]}$. And, let \mathbf{E}_R be an $(N_1 - n_1 + 1)(N_2 - n_2 + 1) \times r$ matrix, where its j^{th} column equals $\mathbf{z}_j^{[N_2-n_2+1]} \otimes \mathbf{w}_j^{[N_1-n_1+1]}$. From (41), we can get the Vandermonde decomposition $\mathcal{H}_2(\mathbf{X})$,

$$\mathcal{H}_2(\mathbf{X}) = \mathbf{E}_L \mathbf{D} \mathbf{E}_R^T,$$

where $\mathbf{D} = \text{diag}([a_1, \dots, a_r])$. Therefore, it verifies that $\mathcal{H}_2(\mathbf{X})$ is rank- r matrix.

Extending from (13), one can check that the corresponding left inverse \mathcal{H}_2^\dagger is defined for each column of \mathbf{X} , by taking average of the anti-diagonals of the Hankel blocks in $\mathcal{H}_2(\mathbf{X})$ corresponding to the same column.